

Minimum Dissipative Relaxed States Applied to Laboratory and Space Plasmas

B. DASGUPTA, DASTGEER SHAIKH, Q. HU and G.P.ZANK

Institute of Geophysics and Planetary Physics (IGPP),
University of California, Riverside, CA 92521. USA.
Email: dastgeer@ucr.edu

(Received April 17 2008, Revised May 6, 2008, Accepted May 7, 2008)

Abstract. The usual theory of plasma relaxation, based on the selective decay of magnetic energy over the (global) magnetic helicity, predicts a force-free state for a plasma. Such a force-free state is inadequate to describe most realistic plasma systems occurring in laboratory and space plasmas as it produces a zero pressure gradient and cannot couple magnetic fields with flow. A different theory of relaxation has been proposed by many authors, based on a well-known principle of irreversible thermodynamics, the principle of minimum entropy production rate which is equivalent to the minimum dissipation rate (MDR) of energy. We demonstrate the applicability of minimum dissipative relaxed states to various self-organized systems of magnetically confined plasma in the laboratory and in the astrophysical context. Such relaxed states are shown to produce a number of basic characteristics of laboratory plasma confinement systems and solar arcade structure.

1. Introduction and Motivation:

Self-organization is a natural process [Ortolani and Schnack, 1993] in which a continuous system evolves toward some preferred states showing a form of order on long scales. Examples of such self-organization processes are ubiquitous in nature and in systems studied in the laboratory. These ordered states are very often remarkably robust, and their detailed structures are mostly independent of the way the system is prepared. The final state to which a system evolves generally depends on the boundary conditions, inherent geometry of the particular device, but is relatively independent of the initial conditions. Self-organization in plasma is generally called Plasma Relaxation. The seminal theory for plasma relaxation first proposed by Taylor (1974) yields a force-free state with zero pressure gradient. Taylor's theory was the first to explain the experimentally observed field reversal of the Reversed Field Pinch (RFP).

Self-organized states with zero pressure gradient are often far from experimentally realizable scenarios. Any realistic magnetic configuration confining plasma must have a non-zero pressure gradient. Extensive numerical simulations [Sato et al., 1996, Zhu et al., 1995] have established the existence of self-organized states of plasma with finite pressure, i.e., these states are observed to be governed by the magnetohydrodynamic force balance equation. Numerical simulations [Dasgupta et al, 1995, Watanabe et al, 1997] and experiments [Ono et al., 1993] have established

that counterhelicity merging of two spheromaks can produce a Field-Reversed Configuration (FRC). The FRC has a zero toroidal magnetic field, and the plasma is confined entirely by poloidal magnetic field. It has a finite pressure, nonzero perpendicular component of current and is more often characterized by a high value of plasma beta. The stability and long life categorize FRC as a relaxed state, which is not obtainable from Taylor model of relaxation. Since spheromaks are depicted as a Taylor state [Rosenbluth and Bussac, 1979], formation of a FRC from the merging of two counterhelicity spheromaks is a unique process from the point of view of plasma relaxation, where a non-force free state (hence non-Taylor state) emerges from the coalescence of two Taylor states. In astrophysical context, particularly solar physics scenario, a 3-D MHD simulation by Amari and Luciano [2000], among others, showed that, after the initial helicity drive, the final “relaxed state is far from the ... linear force-free model that would be predicted by Taylor’s conjecture” and they suggested to derive an alternative variational approach. Such physical processes call for an alternate model for plasma relaxation to broadly accommodate a large number of these observations.

In this context, an important work by Turner deserves special attention. Turner first showed (1986) that a relaxed magnetic field configuration which can support/confine a plasma with a finite pressure gradient. Adopting a two-fluid approach, a model of magnetofluid relaxation is constructed for Hall MHD, under the assumptions of minimum energy (magnetic plus fluid) with the constraints of global magnetic helicity hybrid helicity, axial magnetic flux and fluid vorticity. Euler-Lagrange equations resulted from such variational approach show the coupling between the magnetic field and the fluid vorticity. The solutions for such coupled equations are shown to be achieved by the linear superposition of the eigenvectors of the ‘curl’ operator (force-free states). These solutions yield magnetic field configurations which can confine plasma with a finite pressure gradient.

The principle of “minimum rate of entropy production” formulated by Prigogine and others [Prigogine, 1947] is believed to play a major role in many problems of irreversible thermodynamics. This principle states that for any steady irreversible processes, the rate of entropy production is minimum. For most irreversible processes in nature, the minimum rate of entropy production is equivalent to the minimum rate of energy dissipation. A magnetized plasma is such a dissipative system and it is appropriate to expect that the principle of minimum dissipation rate of energy has a major role to play in a magnetically confined plasma. It is worth mentioning that Rayleigh [1873] first used the term “principle of least dissipation of energy” in his works on the propagation of elastic waves in matter. Chandasekhar and Woltjer [1958] considered a relaxed state of plasma with minimum Ohmic dissipation with the constraint of constant magnetic energy and obtained an equation for the magnetic field involving a ‘double curl’ for the magnetic field and remarked that the solution of such equation is “much wider” than the usual force free solution.

Montgomery and Phillips [1988] first used the principle of minimum dissipation rate (MDR) of energy in an MHD problem to understand the steady the steady profile of a RFP under the constraint of a constant rate of supply and dissipation of helicity with the boundary conditions for a conducting wall. Farengo et al [Farengo et al, 1994,1995, 2002, Bouzat, 2006] in a series of papers applied the principle of MDR to a variety of problems ranging from flux-core spheromak to tokamak.

In this work, we present an alternative scenario for plasma relaxation which is based on the principle of minimum dissipation rate (MDR) rate of energy. This

model gives us a non-force free magnetic field, capable of supporting finite pressure gradient. We demonstrate that this model can reproduce some of the basic characteristics of most of the plasma confining devices in the laboratory as well as the arcade structure of solar magnetic field. A two-fluid generalization of this model for an open system couples magnetic field with flow - so this model is applicable to other astrophysical situations.

The plan of the paper is as follows: In section 2, we present a single fluid MDR model for closed system and briefly discuss its applications to some of the laboratory plasma confinement devices, such as RFP, Spheromak, Tokamak and FRC. We present the result of a recent numerical simulation to justify our choice of the energy dissipation rate as an effective minimizer in our variation problem. In section 3 we describe a generalized version of the MDR model for open two fluid system and its application to solar arcade problem. We summarize a numerical extrapolation method for non-force free coronal magnetic field based on our MDR model. Section 4 concludes our paper.

2. Single fluid MDR based model

To obtain both the field reversal and a finite pressure gradient for RFP, Dasgupta et al. [Dasgupta et al., 1998] considered the relaxation of a slightly resistive and turbulent plasma using the principle of MDR under the constraint of constant global helicity. With the global helicity K_M and the dissipation rate R defined as,

$$K_M = \int_V \mathbf{A} \cdot \mathbf{B} dV; \quad R = \int_V \eta \mathbf{j}^2 dV, \quad (2.1)$$

the variational principle $\delta(R - \Lambda K)$ leads to the following Euler-Lagrange equation,

$$\nabla \times \nabla \times \nabla \times \mathbf{B} = \Lambda \mathbf{B}. \quad (2.2)$$

Solutions of the above equation can be constructed as a superposition of the force free equation using Chandrasekhar-Kendall (CK) eigenfunctions [Chandrasekhar and Kendall, 1957]

$$B = \alpha_1 B_1 + \alpha_2 B_2 + \alpha_3 B_3, \quad (2.3)$$

where $\alpha_1, \alpha_2, \alpha_3$ are constants, to be determined from the boundary conditions, and \mathbf{B}_i 's are obtained from

$$\nabla \times \mathbf{B}_i = \lambda_i \mathbf{B}_i; \quad (i = 1, 2, 3); \quad \lambda_i^3 = \Lambda. \quad (2.4)$$

We have used the analytic continuation of CK eigenfunctions in the complex domain. However, one can easily ascertain that the resulting magnetic field \mathbf{B} is real. Moreover, since the superposition of force free fields with different eigenvalues λ_i is not a force free field, the resultant magnetic field \mathbf{B} is not force free, $\mathbf{J} \times \mathbf{B} \neq 0$. An explicit form of the solution in cylindrical geometry with the boundary conditions for an RFP (perfectly conducting wall) has shown two remarkable features: (1) Such a state can support a pressure gradient; and (2) Field reversal is found in states that are not force free.

In Figure 1 a plot of the field reversal parameter F against the pinch parameter

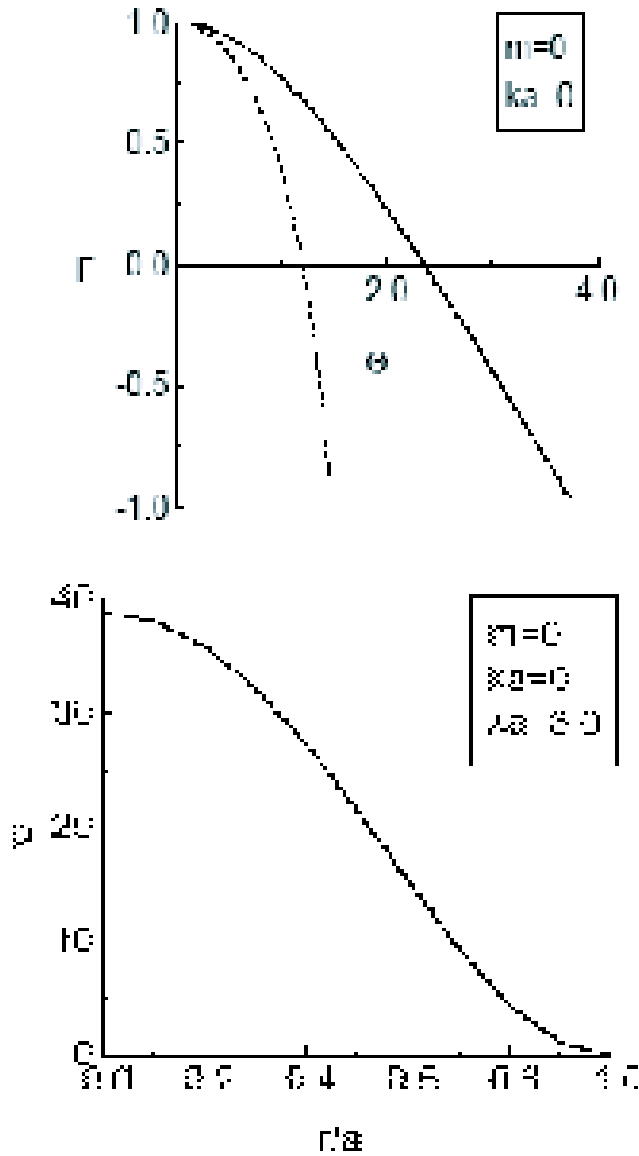


Figure 1. Left panel: Plot of $F = B_z(a)/\langle B_z \rangle$ and $\Theta = B_\theta(a)/\langle B_z \rangle$ ($\langle \dots \rangle$ is the volume average and a is the radial distance) showing the field reversal of RFP obtained from MDR model. The dotted curve represents the plot for the minimum energy state of Taylor. Right Panel: Pressure profile of RFP obtained from MDR model. (from Dasgupta et al., 1998).

Θ is shown. It is found that axial field reverses at a value $\Theta \simeq 2.2$; and the pressure profile of the RFP obtained from our MDR model.

A success of this theory is its applicability in a tokamak configuration [Bhattacharya et al., 2000]. In toroidal geometry, the CK eigenfunctions are hypergeometric functions in the large aspect ratio approximation. Equilibria can be con-

structed under the assumption that the total current $\mathbf{J} = 0$ at the edge. The solution reproduces the q -profile, the toroidal magnetic field, the pressure profile and $\sigma = \mathbf{J} \cdot \mathbf{B} / B^2$ for tokamak, which are very close to the observed profiles (e.g., figure 2). The solutions allow for a tokamak, low- q discharge as well as RFP like behavior with a change of eigenvalue which would essentially determine the amount of volt-sec associated with the discharge characterizing the relaxed state. The poloidal Volt-sec/toroidal flux associated with the discharge can be directly interpreted in terms of the parameter λr_0 (r_0 is the minor radius of the torus, $\lambda = \sqrt[3]{\Lambda}$) and can be shown to increase with λr_0 . MDR relaxed state can yield several kinds of solutions with distinct q -profiles. For low values of λr_0 , the q -profile is monotonically increasing and hence the solutions resemble a tokamak type discharge together with a nearly constant toroidal field, for larger values of λr_0 the toroidal field reverses at the edge, signifying an RFP-type behavior and for intermediate values, the relaxed states indicate an ultra low- q type of discharge exhibiting a q -profile with a pitch minimum and $0 < q < 1$. In figure 2, we plot the toroidal magnetic field B_ϕ , $\sigma = \mathbf{J} \cdot \mathbf{B} / B^2$, q and pressure profiles for different values of λr_0 , for a fixed value of the aspect ratio = 4.0. The continuous line corresponds to $\lambda r_0 = 1.5$, and shows a monotonic increase with r , which is the essential feature of tokamak discharge. For this case the toroidal magnetic field (B_ϕ) is essentially constant and the pressure profile has a peak at the center of the minor cross section of the torus and falls to zero at the edge. A non-constant behavior is shown by the σ profile. The dotted line corresponds to $\lambda r_0 = 3.0$. In this case the toroidal field reverses sign at the edge, which corresponds to an RFP like discharge. The q -profile shows a similar behavior. The σ profile has a dip at $r = 0$ and exhibits a bump near the outer region. Such profiles have been experimentally observed in the ETA-BETA-II device [Antoni et al, 1983]. For the values $\lambda r_0 = 2.5$ the q -profile shows a nonmonotonic behavior as shown in figure 3. The toroidal magnetic field again peaks at the center and slowly decreases towards the edge, showing a paramagnetic behavior that is typical of ultra low- q discharge [Yoshida et al., 1986]. Pressure profile peaks at the center and goes to zero at the edge. Some of these results have been observed in the SINP tokamak [Lahiri et al, 1996] and were also reported earlier in REPUTE-1 [Yoshida et al., 1986] and in TORIUT-6 [Yamada et al, 1987].

This model has been utilized to obtain the spheromak configuration from the spherically symmetric solution under appropriate boundary conditions relevant to an insulating boundary at the edge [Dasgupta et al., 2002]. These boundary conditions are consistent with the classical spheromak solution used by Rosenbluth and Bussac [1979]. The most interesting part of this spheromak solution is the non-constant profile for $\mathbf{J} \cdot \mathbf{B} / B^2$ plotted against normalized distance from the magnetic axis. This profile shows peaks outside the magnetic axis, and this feature is qualitatively closer to the experimentally observed profile reported by Hart et al. [Hart et al., 1983].

The field-reversed configuration (FRC) is a compact toroidal confinement device [Tuszewski, 1988] which is formed with primarily poloidal magnetic field and a zero or negligibly small toroidal magnetic field. The plasma beta of the FRC is one of the highest for any magnetically confined plasma. FRC can be considered as a relaxed state [Guo et al, 2005, 2006], but it is a distinctly non-Taylor state. The FRC configuration can be obtained for an externally driven dissipative system which relaxes with minimum dissipation. In Bhattacharya et al., [2001] we show that

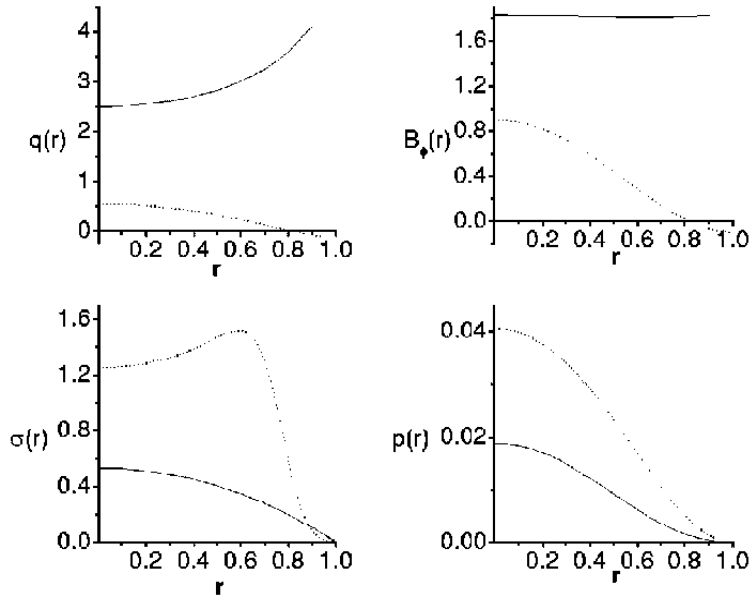


Figure 2. q -profile, B_ϕ , σ , and pressure profile of (i) Tokamak discharge (continuous line); (ii) RFP discharge (dotted line); (from Bhattacharya et al., 2000).

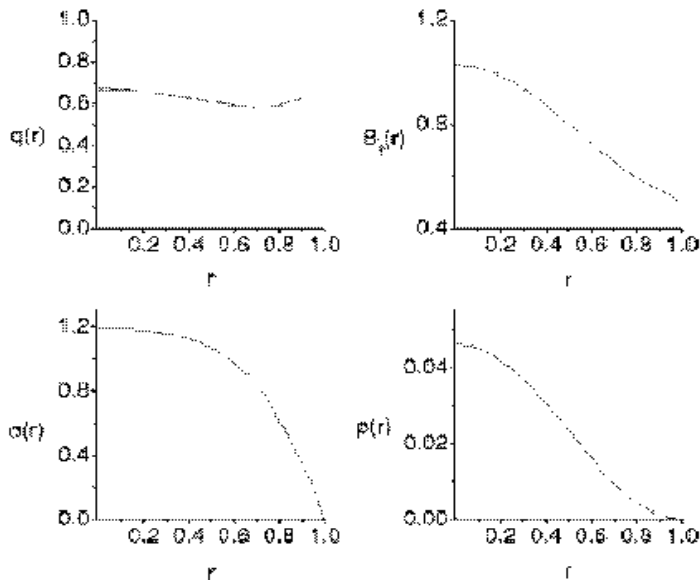


Figure 3. q -profile, B_ϕ , σ , and pressure profile of low- q Discharge; (from Bhattacharya et al., 2000).

the Euler-Lagrange equations for relaxation under MDR with magnetic energy as the constraint represents an FRC configuration for one choice of eigenvalues. This solution is characterized by high beta, zero helicity and a completely null toroidal field and supports a non-constant pressure profile (non-force free). Another choice of eigenvalue leads to a spheromak configuration. A generalization of this work

incorporating flow [Bhattacharya et al., 2003] and taking magnetic and flow energies and cross helicities as constraints also produces the FRC configuration. This state supports field aligned flows with strong shears that may lead to stability and better confinement.

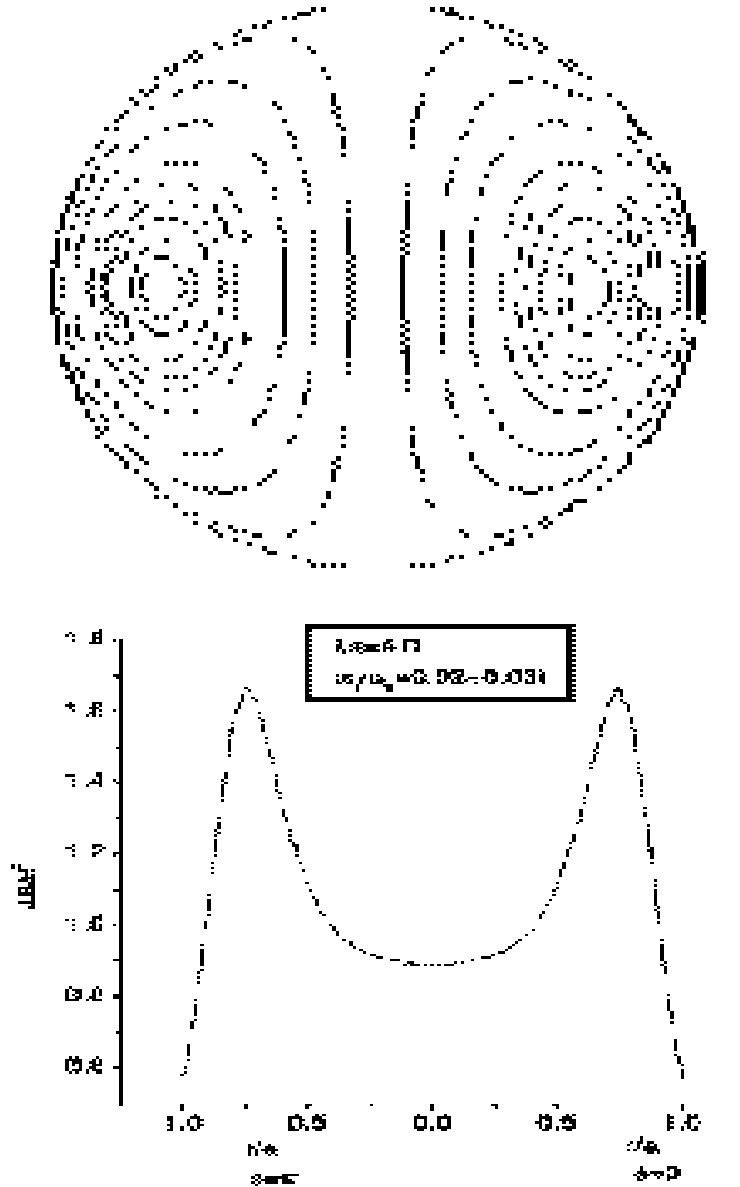


Figure 4. Spheromak configuration (left panel) and the non-constant J_{\parallel}/B derived from our model based on MDR (right panel); (from Dasgupta et al., 2002).

2.1. Simulation Results:

To justify the use of the MDR principle in plasma relaxation and the choice of the total dissipation rate as a minimizer in the variational principle we performed a fully 3-D numerical simulations for a turbulent and slightly dissipative plasma using a fully compressible MHD code [Shaikh et al., 2007] with periodic boundary conditions. Fluctuations are Fourier expanded and nonlinear terms are evaluated in real space. Spectral methods provide accurate representation in Fourier space. In our code there is very little numerical dissipation, and hence the ideal invariants are preserved. The selective decay processes (in addition to dissipation) depend critically on the cascade properties associated with the rugged MHD invariants that eventually govern the spectral transfer in the inertial range. This can be elucidated as follows [Biscamp, 2003]. Magnetic vector potential in 3D MHD dominates, over the magnetic field fluctuations, at the smaller Fourier modes, which in turn leads to a domination of the magnetic helicity invariant over the magnetic energy. On the other hand, dissipation occurs predominantly at the higher Fourier modes which give rise to a rapid damping of the energy dissipative quantity R . A heuristic argument for this process can be formulated in the following way. The decay rates of helicity K and dissipation rate $R = \int_V \eta j^2 dV$ in the dimensionless form, with the magnetic field Fourier decomposed as $\mathbf{B}(\mathbf{k}, t) = \sum_k \mathbf{b}_k \exp(i\mathbf{k} \cdot \mathbf{r})$, can be expressed as,

$$\frac{dK}{dt} = -\frac{2\eta}{S} \sum_k k \mathbf{b}_k^2; \quad \frac{dR}{dt} = -\frac{2\eta^2}{S^2} \sum_k k^4 \mathbf{b}_k^2 \quad (2.5)$$

where $S = \tau_R/\tau_A$, is the Lundquist number, τ_R, τ_A are the resistive and Alfvén time scales, respectively. The Lundquist number in our simulations varies between 10^6 and 10^7 . We find that at scale lengths for which $k \approx S^{1/2}$, the decay rate of energy dissipation is $\sim O(1)$. But at these scale lengths, helicity dissipation is only $\sim O(S^{-1/2}) \ll 1$. This physical scenario is consistent with our 3D simulations. Figure 5 shows the time evolution of the global helicity K_M , total magnetic energy W_M and the total dissipation rate R . It is seen that global helicity remains approximately constant, (decaying very slightly during the simulation time) while the magnetic energy decays faster than the global helicity, but the energy dissipation rate decays even faster than the magnetic energy. The results of the simulation show that total dissipation rate can serve as a minimizer during a relaxation process.

3. MDR based relaxation model for two fluid plasma with external drive:

Recently, Bhattacharya and Janaki [2004] developed a theory of dissipative relaxed states in two-fluid plasma with external drive. We describe the plasma (consisting of ions and electrons) by the two-fluid equations. The basic advantages of a two-fluid formalism over the single-fluid or MHD counterpart are: (i) in a two-fluid formalism, one can incorporate the coupling of plasma flow with the magnetic field in a natural way, and (ii) the two-fluid description being more general than MHD, is expected to capture certain results that are otherwise unattainable from a single-fluid description. It should be mentioned that although we are invoking the principle of minimum dissipation rate of energy - instead of the principle of minimum energy

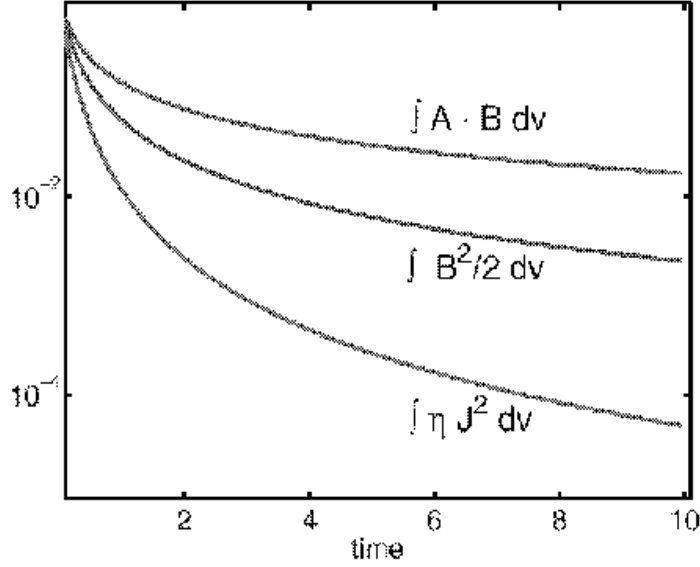


Figure 5. Time evolution of decay rates associated with the turbulent relaxation of the ideal MHD invariants, viz, global magnetic helicity $K_M = \int_V \mathbf{A} \cdot \mathbf{B} dV$, magnetic energy $W = \int_V B^2/2 dV$ and the total dissipation $R = \int_V \eta J^2 dV$, all shown in the same scale.

- our approach is closely similar to the approach to plasma relaxation including Hall terms, as developed by Turner (1986).

In the two-fluid formalism the canonical momentum \mathbf{P}_j canonical vorticity $\mathbf{\Omega}_j$, for the j -th species are defined respectively as,

$$\mathbf{P}_j = m_j \mathbf{u}_j + \frac{q_j}{c} \mathbf{A}, \quad \mathbf{\Omega}_j = \nabla \times \mathbf{P}_j, \quad (j = i, e). \quad (3.1)$$

A gauge invariant expression for the generalized helicity is introduced by defining

$$K_j = \int_V \mathbf{P}_j \cdot \mathbf{\Omega}_j d\tau - \int_V \mathbf{P}'_j \cdot \mathbf{\Omega}'_j dV; \quad (3.2)$$

which is a relative helicity with respect to reference field having \mathbf{P}'_j as the canonical momentum, and \mathbf{P}_α and \mathbf{P}'_α are different inside the volume of interest and the same outside. The gauge invariance condition holds

$$(\mathbf{\Omega}_j - \mathbf{\Omega}'_j) \cdot \hat{n} = 0 \Rightarrow (\mathbf{B} - \mathbf{B}') \cdot \hat{n} = 0 \quad (\omega_j - \omega'_j) \cdot \hat{n} = 0, \quad (\omega_j = \nabla \times \mathbf{u}_j), \quad (3.3)$$

under the condition that there is no flow-field coupling at the surface. The above equations then represent natural boundary conditions inherent to the problem.

The helicity balance equation for the generalized helicity, obtained from the balance equations for the generalized momentum and vorticity, consists of two terms, the helicity injection terms and helicity dissipation term (containing resistivity and viscosity). The global helicity can be taken as a bounded function following Montgomery et al.,(1988) and it is possible to form a variational problem with the helicity dissipation rates as constraints. Thus,

$$\frac{dK_\alpha}{dt} = - \oint [G_\alpha - \mathbf{P}_\alpha \cdot \mathbf{u}_\alpha] \mathbf{\Omega}'_\alpha \cdot \hat{n} da - \oint (\mathbf{P}_\alpha \cdot \mathbf{\Omega}_\alpha) \mathbf{u}_\alpha \cdot \hat{n} da$$

$$\begin{aligned}
& - \oint \left(\frac{\partial \mathbf{P}'_\alpha}{\partial t} \times \mathbf{P}'_\alpha \right) \cdot \hat{n} da - \eta'_\alpha \oint [\{\nabla \times \mathbf{B} + L_\alpha \omega_\alpha\} \times \mathbf{P}_\alpha] \cdot \hat{n} da \\
& - 2\eta'_\alpha \int [\nabla \times (\mathbf{B} + L_\alpha \omega_\alpha)] \cdot \boldsymbol{\Omega}_\alpha d\tau
\end{aligned} \tag{3.4}$$

with

$$\begin{aligned}
G_\alpha &= \left[q_\alpha \phi + \frac{h_\alpha}{n_\alpha} - \frac{m_\alpha u_\alpha^2}{2} \right]; \quad \eta'_\alpha = \frac{q_\alpha \eta c}{4\pi} \\
L_\alpha &= \frac{4\pi}{q_\alpha c n_\alpha} \frac{\mu_\alpha}{\eta} \equiv \text{Prandtl number.}
\end{aligned} \tag{3.5}$$

The minimization integral is then obtained as,

$$\begin{aligned}
\mathcal{I} &= \int \left[(\nabla \times \mathbf{B}) \cdot (\nabla \times \mathbf{B}) + \frac{4\pi n q L_i}{c} \omega_i \cdot \omega_i \right] d\tau \\
&+ \lambda_i \int [\nabla \times (\mathbf{B} + L_i \omega_i)] \cdot \boldsymbol{\Omega}_i d\tau - \lambda_e \int (\nabla \times \mathbf{B}) \cdot \boldsymbol{\Omega}_e d\tau
\end{aligned} \tag{3.6}$$

where $L_i = 4\pi\mu_i/ecn_i\eta$ is the magnetic Prandtl number for ions, μ_i is the ion viscosity and η is the resistivity. We assumed the electron mass $m_e \rightarrow 0$. The first two terms in the above integral represent the ohmic and viscous dissipation rates while the second two integrals represent the ion and electron generalized helicity dissipation rates. λ_i and λ_e are the corresponding Lagrange undetermined multipliers. The Euler-Lagrange equations are written as,

$$\nabla \times \nabla \times \mathbf{B} + \frac{(\lambda_i + \lambda_e)q}{c} \nabla \times \mathbf{B} + \frac{\lambda_i}{2} \left(\frac{qL_i}{c} + m_i \right) (\nabla \times) \omega_i = \nabla \psi; \tag{3.7}$$

$$\nabla \times \nabla \times \omega_i + \frac{2\pi n q}{m_i \lambda_i c} \nabla \times \omega_i + \frac{1}{2m_i L_i} \left(\frac{qL_i}{c} + m_i \right) (\nabla \times)^2 \mathbf{B} = \nabla \chi; \tag{3.8}$$

where ψ and χ are arbitrary gauge functions, with $\nabla^2 \psi = \nabla^2 \chi = 0$. Following Turner (1986) we can write the exact solution of the coupled equations (3.7) and (3.8) as a linear superposition of two CK eigenfunctions, which are the solutions of $\nabla \times \mathbf{Y}_k = \lambda_k \mathbf{Y}_k$ i.e.,

$$\mathbf{B} = \mathbf{Y}_1 + \alpha \mathbf{Y}_2 \quad \omega_i = \mathbf{Y}_1 + \beta \mathbf{Y}_2, \tag{3.9}$$

and α and β are constants and quantify the non force-free part, to be obtained from some boundary conditions.

3.1. Application to solar arcade problem

One of the important features of this formalism is the presence of a nontrivial flow and the coupling between the magnetic field and the flow. The solutions of the corresponding Euler-Lagrange equation highlight the role of nonzero plasma flow in securing a steady MDR relaxed state for an open and externally driven system. This model has been very successful in describing the arcade structures observed in Solar corona [Bhattacharya et al., 2007]. To model solar arcade-type magnetic fields, we make some simplified assumptions and consider a 2-D magnetic field in the x - z plane with the x direction lying on the photosphere surface and z is the vertical direction. With appropriate boundary conditions and after some lengthy algebra, the solutions for the components of the magnetic fields are obtained as,

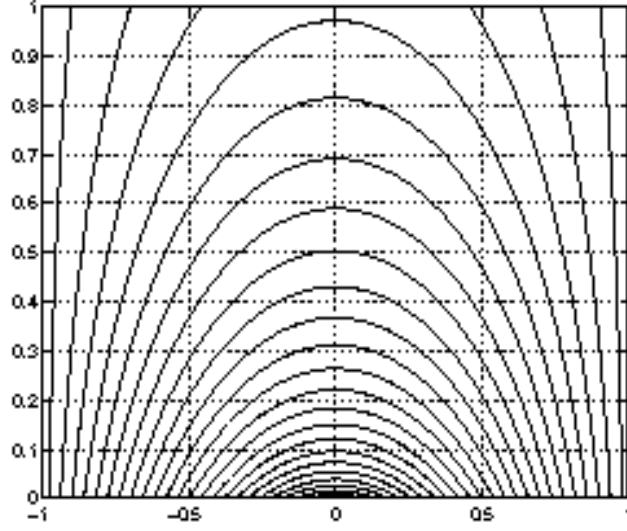


Figure 6. Flow lines in the x - z plane for $\gamma = 1.5$ (from *Bhattacharya et al., 2007*).

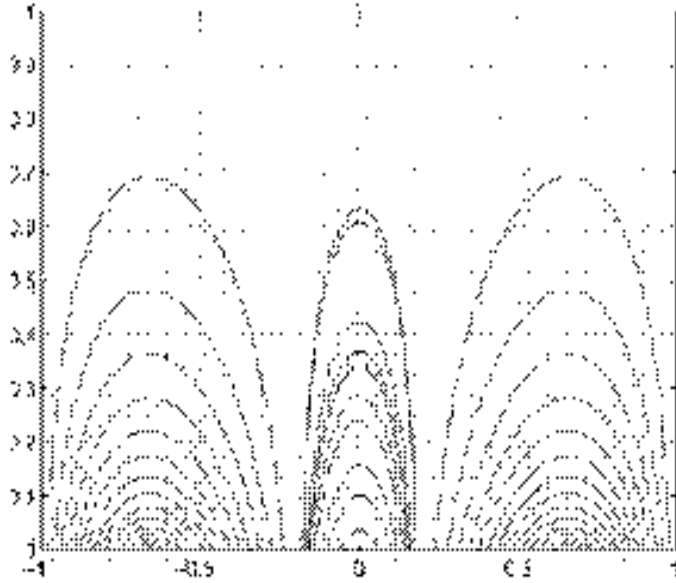


Figure 7. Magnetic field lines in the x - z plane corresponding to (i) single arcade structure for $\gamma = 1.5$ in left panel and (ii) triple arcade structure for $\gamma = 3.36$ in right panel (from *Bhattacharya et al., 2007*).

$$\begin{aligned}
 B_x &= \sqrt{\gamma^2 - 1} \left[2 \cos \gamma x - \frac{2 \cos \gamma}{\cos \sqrt{\gamma^2 - 1}} \cos(x \sqrt{\gamma^2 - 1}) \right] e^{-z \sqrt{\gamma^2 - 1}}; \\
 B_y &= 0;
 \end{aligned}
 \tag{3.10}$$

$$B_z = - \left[2\gamma \sin \gamma x - \frac{2\sqrt{\gamma^2 - 1} \cos \gamma}{\sin \sqrt{\gamma^2 - 1}} \sin(x\sqrt{\gamma^2 - 1}) \right] e^{-z\sqrt{\gamma^2 - 1}};$$

with $\gamma = \sqrt{(k^2 + \lambda^2)}/\lambda^2$ (λ is the eigenvalue and k is the wave number associated with the solution). The same procedures can be adopted for the flow pattern. In figure 7 the magnetic field lines in the x - z plane is plotted for two different values of the parameter γ . The arcade structures are obtained by solving the field line equations $\frac{dz}{dx} = \frac{B_z}{B_x}$. It is interesting to note that the arcade structure changes with the change of the single parameter γ . Figure 6 plots the flow lines for $\gamma = 1.5$. In cylindrical geometry the solutions of eqn. (3.7) can be written in terms of a superposition of Bessel functions. Such solutions yield 3-D Flux ropes, which are plotted in the Figure (8).

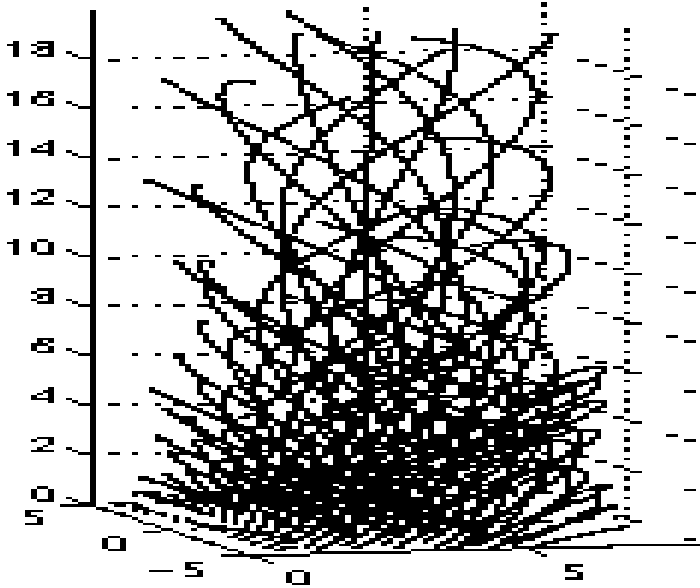


Figure 8. Plot of 3-D Fluxrope obtained from the solution eqn.(3.7).

3.2. Non-force Free Coronal Magnetic Field Extrapolation Based on MDR:

An outstanding problem in solar physics is to derive the coronal magnetic field structure from measured photospheric and/or chromospheric magnetograms. A new approach to deriving three-dimensional non-force free coronal magnetic field configurations from vector magnetograms, based on the MDR principle has been recently developed [Hu, Dasgupta, & Choudhary (2007)]. In contrast to the principle of minimum energy, which yields a linear force-free magnetic field, the MDR gives a more general non-force free magnetic field with flow. The full MDR-based approach requires two layers of vector magnetic field measurements. Its exact solution can be expressed as the superposition of two linear force-free fields with distinct λ parameters, and one potential field. The final solution is thus decomposed into three linear force-free extrapolations, with bottom boundary conditions derived from the measured vector magnetograms, at both photospheric and chromospheric levels. The semi-analytic test case shown in Figure 9 illustrates the feasibility and the high

performance of this method. This extrapolation is easy to implement and much faster than most other nonlinear force-free methods [Hu & Dasgupta 2007]. It also takes full advantage of multiple layer solar magnetic field measurements, thus gives a more realistic result.

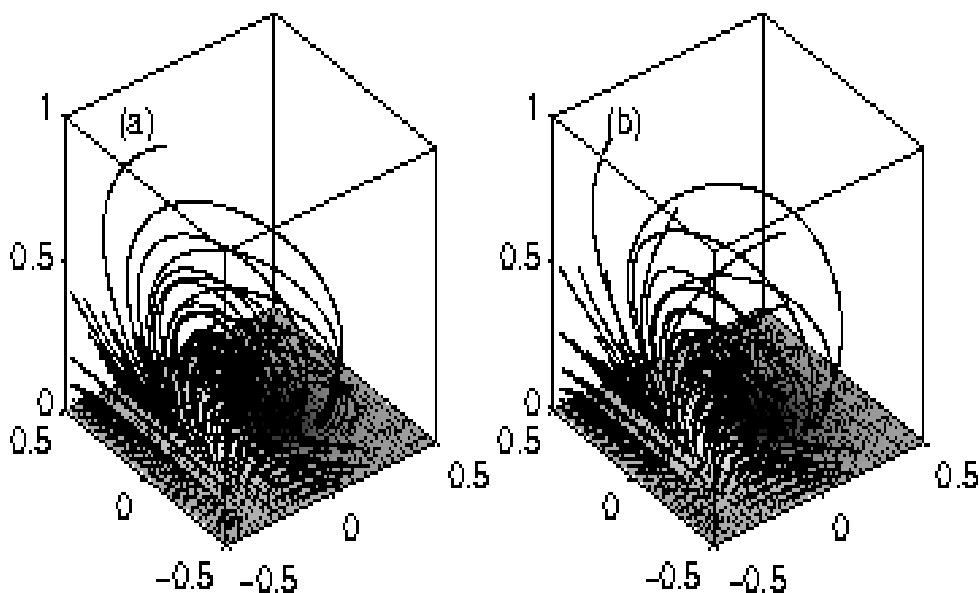


Figure 9. 3D view of magnetic field lines in a box simulating the typical extrapolation domain. (a) exact solution; (b) numerical extrapolation result. Bottom image at height 0 shows the normal field component distribution with gray scale indicating strongly negative (black) to positive (white) field. The great resemblance between the exact and the numerical solutions justifies the feasibility and high performance of this method (Hu, Dasgupta, & Choudhary 2007).

4. Conclusion

We have demonstrated that a relaxation model based on the minimum dissipation of energy can successfully explain some of the salient observations both in laboratory and space plasma. An MDR based model in its simpler form is capable of yielding basic characteristics of most of the laboratory plasma confinement devices, and a generalization of this model for two fluid with external drive can couple magnetic field and flow and predict solar arcade structures. The above findings definitely points out that the MDR relaxed states applied to astrophysical plasmas is a worthy case for further investigations. In future we plan to apply this model to investigate magnetic field structure in the sun with an aim to understanding coronal mass ejection.

5. Acknowledgement

We gratefully acknowledge partial supports from NASA LWS grant NNX07A073G, and NASA grants NNG04GF83G, NNG05GH38G, NNG05GM62G, a Cluster Uni-

versity of Delaware subcontract BART372159/SG, and NSF grants ATM0317509, and ATM0428880.

References

- [1] Amari, T., and Luciani, J. F., Phys. Rev. Letts., **84**, 1196, (2000)
- [2] Antoni, V., S. Martini, S. Ortolini and R. Paccagnella, in *Workshop on Mirror-based and Field-reversed approaches to Magnetic Fusion*, Int. School of Plasma Physics, Varenna, Italy, p. 107, (1983)
- [3] Bhattacharya, R., M.S. Janaki and B. Dasgupta, Phys. Plasmas,**7**, 4801, (2000)
- [4] Bhattacharya, R., M.S. Janaki and B. Dasgupta, Phys. Lett. A , **291A**, 291, (2001)
- [5] Bhattacharyya, R., M. S. Janaki and B. Dasgupta, Plasma Phys. Contr. Fusion, **45**, 63 (2003).
- [6] Bhattacharya, R., and M. S. Janaki, Phys. Plasmas, **11**, 5615 (2004)
- [7] Bhattacharya, R., M. S. Janaki, B. Dasgupta, G. P. Zank, Solar Phys. **240**, 63, (2007)
- [8] Biskamp, D. 2003, Magnetohydrodynamic Turbulence, *Cambridge University Press*.
- [9] Bouzat, S. and R. Farengo, J. Plasma Phys., **72**, 443, (2006)
- [10] Chandrasekhar, S. & P. C. Kendall, Astrophys. J., **126**, 457 (1957).
- [11] Chandrasekhar, S. & L. Woltjer, Proc. Natl. Acad. Sci. USA, **44**, 285 (1958).
- [12] Dasgupta, B., T. Sato, T Hayashi, K. Watanabe and T-H Watanabe, Trans. Fusion Tecnol., **27**, 374, (1995)
- [13] Dasgupta, B., P. Dasgupta, M. S. Janaki, T. Watanabe and T. Sato, Phys. Rev. Lett., **81**, 3144, (1998)
- [14] Dasgupta, B., M. S. Janaki, R. Bhattacharya, P. Dasgupta, T. Watanabe, and T. Sato, Phys. Rev. E , **E 65**, 046405, (2002)
- [15] Farengo, R. and J. R. Sobehart, Plasma Phys. Contr. Fus., **36**, 465 (1994)
- [16] Farengo, R. and J. R. Sobehart. Phys. Rev. E, **52**, .2102 (1995)
- [17] Farengo, R. and K. I. Caputi, Plasma Phys. Contr. Fus., **44**, 1707 (2002)
- [18] Guo, H. Y., A. L. Hoffman, L. C. Steinhauer, and K. E. Miller, Phys. Rev. Letts, **95**. 175001, (2005)
- [19] Guo, H. Y., A. L. Hoffman, L. C. Steinhauer, K. E. Miller, and R. D. Milroy, Phys. Rev. Letts, **97**. 175001, (2006)
- [20] Hu, Q., Dasgupta, B., & Choudhary, D.P. 2007, AIP CP, **932**, 376, (2007)
- [21] Hu, Q., and Dasgupta, B. , *Sol. Phys.*, **247**, 87, (2008)
- [22] Hart, G. W., C. Chin-Fatt, A. W. deSilva, G. C. Goldenbaum, R. Hess and R. S. Shaw, Phys. Rev. Lett., **51**, 1558, (1983)
- [23] Lahiri, S., A. N. S. Iyenger, S. Mukhopadhyay and R. Pal, Nucl. Fusion, **36**, 254, (1996)
- [24] Montgomery D. and L. Phillips, Phys. Rev. A, **38**, 2953 (1988)
- [25] Ono, Y., A. Morita, and M. Katsurai and M Yamada, Phys. Fluids, **B5**, 3691, (1993)
- [26] Ortolani, S. and D. D. Schnack, Magnetohydrodynamics of plasma relaxation, *World Scientific*, (1993)

- [27] Prigogine, I., *Etude Thermodynamique des Phénomènes Irreversibles*, Editions Desoer, Liège, (1946)
- [28] Rayleigh, Proc. Math Soc. London, **363**, 357 (1873)
- [29] Rosenbluth, M. N. and M. N. Bussac, Nucl. Fusion, **19**, 489, (1979)
- [30] Sato, T. and Complexity Simulation Group: S. Bazdenkov, B. Dasgupta, S. Fujiwara, A. Kageyama, S. Kida, T. Hayashi, R. Horiuchi, H. Muira, H. Takamaru, Y. Todo, K. Watanabe and T.-H. Watanabe, Phys. Plasmas, **3**, 2135 (1996)
- [31] Shaikh, D., B. Dasgupta, G. P., Zank, and Q. Hu, *Phys. Plasmas*, **15**, 012306, (2008)
- [32] Taylor, J. B., Phys. Rev. Lett. **33**, 139 (1974)
- [33] Turner, L., IEEE Trans. Plasma Sc. **14**, 849, (1986)
- [34] Tuszewski, M., Nuc. Fusion, **28**, 2033, (1988)
- [35] Watanabe, T.-H., T. Sato, and T. Hayashi, Phys. Plasmas **4**, (1997)
- [36] Yamada, H., K. Kusano, Y. Kamada, H. Utsumi, Z. Yoshida and N. Inoue, Nucl. Fusion, **27**, 1169, (1987)
- [37] Yoshida, Z., S. Ishida, K. Hattori, Y. Murakami and J. Morikawa, J. Phys. Soc. Jpn., **55**, 554, (1986)
- [38] Zhu, S., R. Horiuchi, and T. Sato, Phys. Rev. E, **51**, 6047 (1995).

L^AT_EX 2_ε Input Guide for Authors

CAMBRIDGE T_EX-T_O-T_YP_E†

(Received 26 July 2003)

Abstract. This guide is for authors who are preparing papers for the *Journal of Plasma Physics* using the L^AT_EX 2_ε document preparation system and the Cambridge University Press JPP class file.

CONTENTS

1. Introduction	2
1.1. Introduction to L ^A T _E X	2
1.2. General style issues	2
1.3. Submission of L ^A T _E X articles	2
1.4. The JPP document class	3
2. Using the JPP class file	3
2.1. Document class options	3
2.2. Additional ‘packages’ supplied with <code>jpp.cls</code>	4
3. Additional facilities	4
3.1. Titles, authors’ names and running headlines	4
3.2. Abstract	5
3.3. Lists	5
3.4. Theorem environments	6
3.5. Definitions	7
3.6. Proof environment	7
4. Mathematics and units	8
4.1. Numbering of equations	8
4.2. AMS fonts – especially if you do not have them	9
4.3. Typeface	10
4.4. Skewing of accents	11
4.5. Units of measure	12
5. User-defined macros	12
6. Some guidelines for using standard facilities	12
6.1. Sections	13
6.2. Tables	13
6.3. Illustrations (or figures)	14
6.4. Acknowledgments	15
6.5. Appendices	15
6.6. References	15
Appendix A	19
Appendix B	20

† Example of thanks

1. Introduction

The layout design for the *Journal of Plasma Physics* has been implemented as a L^AT_EX 2_ε class file. The JPP class is based on the ARTICLE class as discussed in the L^AT_EX manual (2nd edition). Commands which differ from the standard L^AT_EX interface, or which are provided in addition to the standard interface, are explained in this guide. This guide is not a substitute for the L^AT_EX manual itself.

Note that the final printed version of papers will use the Monotype Modern typeface rather than the Computer Modern available to authors. Also, the measure in JPP class is different from L^AT_EX 2_ε article class. For these reasons line lengths and page breaks will change and authors should not insert hard breaks in their text.

1.1. Introduction to L^AT_EX

The L^AT_EX document preparation system is a special version of the T_EX typesetting program. L^AT_EX adds to T_EX a collection of commands which allow the author to concentrate on the logical structure of the document rather than its visual layout.

L^AT_EX provides a consistent and comprehensive document preparation interface. L^AT_EX can automatically number equations, figures, tables, and list entries, as well as sections and subsections. Using this numbering system, bibliographic citations, page references and cross-references to any other numbered entity (e.g. section, equation, figure, list entry) are quite straightforward.

1.2. General style issues

Use of L^AT_EX defaults will result in a pleasing uniformity of layout and font selection. Authors should resist the temptation to make *ad hoc* changes to these. Also avoid use of direct formatting unless really necessary. Papers will be edited as usual, and this process may be obstructed by the use of inserted line breaks, etc.

For general style issues, authors are referred to the ‘Preparation of manuscripts’ in the back cover of the journal. The language used in the journal is British English, and spelling should conform to this.

Use should be made of symbolic references (`\ref`) in order to protect against late changes of order, etc.

1.3. Submission of L^AT_EX articles

Authors who intend to submit a L^AT_EX article should obtain a copy of the JPP class file. This is available by anonymous FTP from

`ftp.cup.cam.ac.uk`

You will find the class file and instructions contained in a single zip archive `jpp-cls.zip` in the directory

`pub/texarchive/journals/latex/jpp-cls`

The `readme.txt` (which is the same directory) tells you how to unzip the `jpp-cls.zip` file. There may also be an ‘unpacked’ directory containing all of the files separately, in case of difficulty. If you cannot obtain the JPP files, use the standard `article` class, with the default ‘10pt’ option.

When submitting the final article, ensure that the following are included and are clearly labelled.

- (a) A hardcopy printout of the article.

- (b) The input file (exactly matching the hardcopy).
- (c) A copy of any user-defined macros.
- (d) If you have used L^AT_EX, the .bib, .bbl and .bst files that were used.
- (e) Any other files necessary to prepare the article for typesetting.

The files for the *final* article should be supplied on a PC or Macintosh disk. Please write on the disk what format it is, as this saves time. Submit the hardcopy and disk by post in the normal way.

1.4. The JPP document class

The use of document classes allows a simple change of style (or style option) to transform the appearance of your document. The CUP JPP class file preserves the standard L^AT_EX interface such that any document which can be produced using the standard L^AT_EX ARTICLE class can also be produced with the JPP class. However, the measure (or width of text) is slightly different from that for ARTICLE; therefore line breaks will change and it is possible that equations may need re-setting.

2. Using the JPP class file

First, copy the file `jpp.cls` and `upmath.sty` (see §2.2) into the correct subdirectory on your system. The JPP document style is implemented as a complete document class, and *not* a document class option. In order to use the JPP class, replace `article` by `jpp` in the `\documentclass` command at the beginning of your document:

```
\documentclass{article}
```

is replaced by

```
\documentclass{jpp}
```

Some of the standard document class options should be used. Author-defined macros should be inserted before `\begin{document}`, or in a separate file and should be included with the submission, see §5. Authors must not change any of the macro definitions or parameters in `jpp.cls`.

2.1. Document class options

In general, the following standard document class options should *not* be used with the JPP class file:

- `10pt`, `11pt` and `12pt` – unavailable;
- `twoside` is the default (`oneside` is disabled);
- `onecolumn` is the default (`twocolumn` is disabled);
- `titlepage` is not required and is disabled;
- `fleqn` and `leqno` should not be used, and are disabled.

The standard document class options should *not* be used with the JPP class:

- `10pt`, `11pt`, `12pt` – unavailable.
- `draft`, `twoside` (no associated class file) – `twoside` is the default.
- `fleqn`, `leqno`, `titlepage`, `twocolumn` – unavailable.

2.2. Additional ‘packages’ supplied with `jpp.cls`

The following additional package (`.sty`) files are supplied in the JPP distribution:

- `upmath` – provides ‘upright’ Greek math characters. Requires the AMS `amsbsy` and `amsgen` packages.

If your site does not have the AMS Fonts and AMS L^AT_εX packages installed, we strongly recommend that your site installs them. With them, you can produce output which is much closer to the final result. The latest AMS Fonts/AMS L^AT_εX distributions can be found on your nearest CTAN (Comprehensive T_εX Archive Network) site.

2.2.1. The UPMATH package The `upmath` package defines the macros `\mathup` and `\mathbup`, which allow access to the symbols in the AMS Euler fonts.

The `upmath` package provides macros for upright lower-case Greek (`\ualpha`–`\uxi`), and for bold lower-case Greek (`\ubalpha`–`\ubxi`). The bold upright symbol `\eta` has to be treated differently, in this case use `\uboldeta`. The `upmath` package also provides `\upartial` and `\ubpartial`.

To use the `upmath` package, you need to have the AMS `eurm/b` fonts installed.

3. Additional facilities

In addition to all the standard L^AT_εX design elements, the JPP class file includes the following features:

- Extended commands for specifying a short version of the title and author(s) for the running headlines.
- Abstract environment
- Control of enumerated lists.
- An extended `theorem` environment, enabling you to also typeset unnumbered theorems, etc.
- Ability to create new theorem-like environments for claims, conjectures, examples, problems, remarks, etc.
- The `subequations` and `subeqnarray` environments for sub-numbering equations.
- A `proof` environment.
- A `acknowledgements` environment.

Once you have used these additional facilities in your document, it can be processed only with `jpp.cls`.

3.1. Titles, authors’ names and running headlines

In the JPP class, the title of the article and the author’s name (or authors’ names) are used both at the beginning of the article for the main title and throughout the article as running headlines at the top of every page. The title is used on odd-numbered pages (rectos) and the author’s name (with initials only for first names) appears on even-numbered pages (versos). The `\pagestyle` and `\thispagestyle` commands should *not* be used. Similarly, the commands `\markright` and `\markboth` should not be necessary.

Although the article title can run to several lines of text, the running headline must be a single line. Moreover, the title can also incorporate new line commands (e.g. `\`) but these are not acceptable in a running headline. To enable you to specify an alternative short title and author’s name, the standard `\title` and `\author`

commands have been extended to take an optional argument to be used as the running headline:

```
\title[A short title]{The full title which can be as long
                        as necessary}
\author[Initials and last names of all authors]{The full names of
        all the authors, using letterspacing and \and before
        the last name in the list}
\affiliation{Author's affiliation}
```

Unlike most other document classes, `jpp.cls` does not follow the convention of using the second line of the `\author` command to write the author's affiliation. Rather, this must be entered using the `\affiliation` command as shown above. The `\and` command does not produce separate author/affiliation pairs, but only generates the word 'and' in small caps as required by the JPP class. Use the predefined macro `\ls` to get the letterspacing between the letters of the author's name. If there is more than one affiliation, use `\\[\affilskip]` between lines of the `\affiliation`, inserting footnote numbers manually.

An example will make all this clearer. To produce

Interesting title

ALAN N. OTHER¹ and J. Q. PUBLIC²

¹University of Moscow, Moscow, Russia

²Ngonga University, Nairobi, Kenya

(Received 12 June 1992)

you would type

```
\title[Short title]{Interesting title}
\author[A. N. Other and J. Q. Public]
        {A\ls L\ls A\ls N\ls N.\ns O\ls T\ls H\ls E\ls R$^1$\ns
        \and\ns J.\,Q.\ns P\ls U\ls B\ls L\ls I\ls C$^2$}
\affiliation{$^1$University of Moscow, Moscow, Russia\\[\affilskip]
             $^2$Ngonga University, Nairobi, Kenya}
\date{12 June 1992}
```

The L^AT_EX `\thanks` command can be used inside the `\author` command to insert an authors 'Current address' information as a footnote, appearing at the bottom of the title page.

3.2. Abstract

The JPP class provides for an abstract, produced by

```
\begin{abstract}
...
\end{abstract}
```

This should appear just *before* the first `\section` command.

3.3. Lists

The JPP style provides the three standard list environments plus an additional unnumbered list:

- Numbered lists, created using the `enumerate` environment.

- Bulleted lists, created using the `itemize` environment.
- Labelled lists, created using the `description` environment.

The `enumerate` environment numbers each list item with an italic letter in parentheses; alternative styles can be achieved by inserting a redefinition of the number labelling command after the `\begin{enumerate}`. For example, a list numbered with roman numerals inside parentheses can be produced by the following commands:

```
\begin{enumerate}
\renewcommand{\theenumi}{\roman{enumi}}
\item first item
:
\end{enumerate}
```

This produces the following list:

- (i) first item
- (ii) second item
- (iii) etc.

In the last example, the item alignment is uneven because the standard list indentation is designed to be sufficient for arabic numerals rather than the wider roman numerals. In order to enable different labels to be used more easily, the `enumerate` environment in the JPP style can be given an optional argument which (like a standard `thebibliography` environment) specifies the *widest label*. For example,

- (i) first item
- (ii) second item
- (iii) etc.

was produced by the following input:

```
\begin{enumerate}[(iii)]
\renewcommand{\theenumi}{\roman{enumi}}
\item first item
:
\end{enumerate}
```

Once you have used the optional argument on the `enumerate` environment, do not process your document with a standard L^AT_EX class file.

3.4. Theorem environments

The `\newtheorem` command works as described in the L^AT_EX manual, but produces spacing and caption typefaces required to the JPP style. The preferred numbering scheme is for theorems to be numbered within sections, as 1.1, 1.2, 1.3, etc., but other numbering schemes are permissible and may be implemented as described in the L^AT_EX manual. In order to allow authors maximum flexibility in numbering and naming, *no* theorem-like environments are defined in `jpp.cls`. Rather, you have to define each one yourself. Theorem-like environments include Theorem, Definition, Lemma, Corollary, and Proposition. For example,

```
\newtheorem{lemma}{Lemma}[section]
```

```
\renewcommand{\thelemma}{\Roman{lemma}}
```

The new macro which follows can also produce numbered and unnumbered environments.

3.5. Definitions

The `\newdefinition` command can be used to create environments for claims, conjectures, examples, problems, remarks, etc. These are typeset in the way as theorems, except the text is typeset in roman instead of italic.

You can have an environment created by `\newdefinition` number in the same sequence as a ‘Theorem’ by adding the optional `[theorem]` argument as below:

```
\newdefinition{definition}[theorem]{Definition}
:
\begin{definition}
This is a definition.
\end{definition}
\begin{definition*}
This is an unnumbered definition.
\end{definition*}
```

which produces the following:

Definition 3.1. This is a definition.

Definition. This is an unnumbered definition.

3.6. Proof environment

The standard L^AT_EX constructs do not include a proof environment to follow a theorem, lemma etc. (see also §3.4), and so one has been added for the JPP style.

Note the use in the following examples of an optional argument in square braces which may contain any information you may wish to add. For example,

```
\begin{theorem}[2]\label{thenv}
Let the scalar function  $T(x,y,t,\mathbf{\omega})$  be a conserved
density for solutions of  $(9)$ . Then the two-component function
\begin{equation}
\mathbf{P} = \mathbf{J} \mathcal{E} T
\end{equation}
represents the infinitesimal generator of a symmetry group
for  $(9)$ .
\end{theorem}
\begin{proof}[Proof of Theorem~\ref{thenv}]
The assumption about  $T$  means that
\[
0 \sim \frac{\partial T}{\partial t} + \mathcal{E} T \mathbf{\omega}_t
= \frac{\partial T}{\partial t} + \{ T, H \},
\]
where  $\frac{\partial T}{\partial t}$  refers to explicit
dependence on  $t$ . The skew symmetry of  $\mathbf{J}$  hence implies
\begin{equation}
```

```
\frac{\partial T}{\partial t} \sim \{ H, T \},
\end{equation}
```

whereupon the operation $\mathcal{J}\mathcal{E}$, which commutes with ∂_t in its present sense, gives

```
\[
\frac{\partial \mathbf{P}}{\partial t}
= \mathcal{J}\mathcal{E}\{ H, T \}.
\]
```

This equation reproduces the characterisation of symmetries that was expressed by (19), thus showing \mathbf{P} to represent a symmetry group.

```
\end{proof}
```

produces the following text:

THEOREM 3.2 (2). *Let the scalar function $T(x, y, t, \omega)$ be a conserved density for solutions of (9). Then the two-component function*

$$\mathbf{P} = \mathcal{J}\mathcal{E}T \tag{3.1}$$

represents the infinitesimal generator of a symmetry group for (9).

Proof. [Proof of Theorem 3.2] The assumption about T means that

$$0 \sim \frac{\partial T}{\partial t} + \mathcal{E}T\omega_t = \frac{\partial T}{\partial t} + \{T, H\},$$

where $\partial T/\partial t$ refers to explicit dependence on t . The skew symmetry of \mathcal{J} hence implies

$$\frac{\partial T}{\partial t} \sim \{H, T\}, \tag{3.2}$$

whereupon the operation $\mathcal{J}\mathcal{E}$, which commutes with ∂_t in its present sense, gives

$$\frac{\partial \mathbf{P}}{\partial t} = \mathcal{J}\mathcal{E}\{H, T\}.$$

This equation reproduces the characterisation of symmetries that was expressed by (19), thus showing \mathbf{P} to represent a symmetry group. \square

The final \square will not be included if the `proof*` environment is used.

4. Mathematics and units

The JPP class file will insert the correct space above and below displayed maths if standard L^AT_EX commands are used; for example use `\[... \]` and *not* `$$... $$`. Do not leave blank lines above and below displayed equations unless a new paragraph is really intended.

4.1. Numbering of equations

The `subequations` and `subeqnarray` environments have been incorporated into the JPP class file. Using these two environments, you can number your equations (1.1a), (1.1b) etc. automatically. For example, you can typeset

$$a_1 \equiv (2\Omega M^2/x)^{\frac{1}{4}}y^{\frac{1}{2}} \tag{4.1a}$$

and

$$a_2 \equiv (x/2\Omega)^{\frac{1}{2}} k_y / M. \quad (4.1b)$$

by using the `subequations` environment as follows:

```
\begin{subequations}
\begin{equation}
a_1 \equiv (2\Omega M^2/x)^{\frac{1}{4}} y^{\frac{1}{2}}
\end{equation}
and
\begin{equation}
a_2 \equiv (x/2\Omega)^{\frac{1}{2}} k_y / M.
\end{equation}
\end{subequations}
```

You may also typeset an `array` such as:

$$\dot{X} = \gamma X - \gamma \delta \eta, \quad (4.2a)$$

$$\dot{\eta} = \frac{1}{2} \delta + 2X\eta. \quad (4.2b)$$

by using the `subeqnarray` environment as follows:

```
\begin{subeqnarray}
\dot{X} & = & \gamma X - \gamma \delta \eta , \\
\dot{\eta} & = & \frac{1}{2} \delta + 2X\eta .
\end{subeqnarray}
```

4.2. AMS fonts – especially if you do not have them

If you need AMS symbols but do not have the AMS fonts you can ensure that they will be correctly typeset by taking the following steps. Set up user-defined macros that can be redefined by the typesetter to use the correct AMS macros. For example, the blackboard bold symbols, sometimes called shell or outline characters, are obtained with the AMS macro `\mathbb{. .}`. Instead, use a macro definition such as:

```
% replace font!
\newcommand\BbbE{\ensuremath{\mathsf{E}}} % Blackboard bold E
```

This substitutes a sans serif character where you want blackboard bold. You can typeset the input file and the typesetter is alerted to do the substitution.

The following example (which uses the `\providecommand` macro) will work without modification by the typesetter, because the `\providecommand` macro will not overwrite any existing `\mathbb` definition.

```
\providecommand\mathbb[1]{\ensuremath{\mathsf{#1}}}
...
\newcommand\BbbE{\mathbb{E}} % Blackboard bold E
```

Plain \TeX provides only `\leq` and `\geq` which typeset the Computer Modern symbols \leq and \geq , respectively. These will be redefined at typesetting to use the AMS symbols `\leqslant` and `\geqslant`, to give the slanted symbols.

If you wish to use AMS fonts with $\LaTeX 2_{\epsilon}$ you must be using at least version 2.0. Earlier versions are not supported.

4.3. Typeface

Sometimes, non-italic symbols are required in maths. This section describes how these may be obtained using L^AT_EX and `jpp.cls`.

4.3.1. Roman symbols The mathematical operators and constants, such as `\sin`, `\cos`, `\log` and `\exp` (and many others) are covered by L^AT_EX 2_ε macros which ensure that they are typeset in roman text, even in math mode: `\sin`, `\cos`, `\log`, `\exp`. Where single letters are concerned (e.g. `d`, `i`, `e`) just use `\mathrm` in math mode, i.e. `\E=m\mathrm{c}^2` which typesets as $E = mc^2$, giving the correct roman character but with math spacing. When the term involves more than one character (e.g. `Re` or `Im`) text-character spacing is required:

```
\mbox{Re}\;x
```

which typesets as $\text{Re } x$.

Where such expressions are used repeatedly, macro definitions can reduce typing and editing. The following examples are included in the preamble of the input files for this document, `jppguide.tex`, and of the sample article `jppsampl.tex`. Authors are encouraged to use them and others like them.

```
\newcommand\Real{\mbox{Re}} % do not confuse with TeX's \Re
\newcommand\Imag{\mbox{Im}} % do not confuse with TeX's \Im
\newcommand\Ai{\mbox{Ai}}
\newcommand\Bi{\mbox{Bi}}
```

4.3.2. Multiletter italic symbols If multiletter symbols are used in maths mode, for example Reynolds, Prandtl numbers, etc. the standard maths mode spacing between them is too large and text-character spacing is required. As described in §4.3.1 (but here for italic letters) use for example

```
\newcommand\Rey{\mbox{\textit{Re}}}
\newcommand\Pran{\mbox{\textit{Pr}}}
```

4.3.3. Upright and sloping Greek symbols Like the italic/roman fonts described above, Greek letters for math variables are printed in the Journal in sloping type, whereas constants, operators and units are upright. However, L^AT_EX normally produces sloping lowercase Greek and upright capitals. The upright lowercase required for example for ‘`\pi`’ and ‘`\mu`’ (micro) are provided by the `upmath` package (from the AMS Euler fonts). If you don’t have the AMS font set, you will have to use the normal math italic symbols and the typesetter will substitute the corresponding upright characters.

You will make this much easier if you can use the macros `\upi` and `\umu` in your text to indicate the need for the upright characters, together with the following definitions in the preamble, where they can easily be redefined by the typesetter.

```
\providecommand\upi{\pi}
\providecommand\umu{\mu}
```

Notice the use of `\providecommand`, this stops your definitions overwriting the ones used by the typesetter.

Sloping uppercase Greek characters can be obtained by using the `\varGamma` etc. macros (which are built into the class file). The few required upright Greek capital letters (e.g. capital delta for ‘difference’) are given by the relevant L^AT_EX macro, e.g. `\Delta`.

4.3.4. Sans serif symbols The `\textsf` and `\mathsf` commands change the typeface to sans serif, giving upright characters. Occasionally, bold-sloping sans serif is needed. You should use the following supplied macros to obtain these fonts.

<code>\textsf{text}</code>	→	text	<code>\mathsf{math}</code>	→	math
<code>\textsf{i}{text}</code>	→	<i>text</i>	<code>\mathsf{i}{math}</code>	→	<i>math</i>
<code>\textsf{b}{text}</code>	→	text	<code>\mathsf{b}{math}</code>	→	math
<code>\textsf{bi}{text}</code>	→	<i>text</i>	<code>\mathsf{bi}{math}</code>	→	<i>math</i>

You can use them like this:

```
\newcommand\ssC{\mathsf{C}} % for sans serif C
\newcommand\sfsP{\mathsf{i}{P}} % for sans serif slanted P
\newcommand\sfbSX{\mathsf{b}{X}} % for sans serif bold slanted X
```

Note that the bold-slanted font `\textsf{bi}` and `\mathsf{bi}` use the slanted sans serif font `cmssi` – because there is no bold-slanted maths sans serif font in Computer Modern! If you use the supplied sans-serif text and math commands the typesetter will be able to substitute the fonts automatically.

4.3.5. Bold math italic symbols If you require bold math italic symbols/letters, L^AT_EX provides several ways of getting them. Firstly, L^AT_EX’s `\boldmath` switch which can be used like this:

```
$ \mbox{\boldmath $P$} = \mathsf{J}\mathcal{E} T $
```

As you can see it takes quite a lot of typing to achieve a bold math italic P. Another problem is that you can’t use `\boldmath` in math mode, thus the `\mbox` forces the resulting text into text style (which you may not want).

You can cut down on the typing by defining the following macro (which is in the preamble of this guide):

```
\providecommand\boldsymbol[1]{\mbox{\boldmath $#1$}}
```

Then for the above example you can define:

```
\newcommand\bldP{\boldsymbol{P}}
```

to achieve the same result. This still doesn’t remove the default to text style problem.

If you have the `amsbsy` package on your system, then you can remove this limitation as well by placing a `\usepackage{amsbsy}` after the `\documentclass` line in your document, and then use `\boldsymbol` for bold math italic symbols (don’t define `\boldsymbol` yourself when using `amsbsy`).

4.3.6. Script characters Script characters should be typeset using L^AT_EX 2_ε’s `\mathcal` command. This produces the Computer Modern symbols such as \mathcal{E} and \mathcal{F} in your hard copy but the typesetter will substitute the more florid script characters normally seen in the journal.

4.4. Skewing of accents

Accents such as hats, overbars and dots are normally centred over letters, but when these are italic or sloping greek the accent may need to be moved to the right so that it is centred over the top of the sloped letter. For example, `\newcommand\hatp{\skew3\hat{p}}` will produce \hat{p} .

4.5. Units of measure

Numbers and their units of measure should be typeset with fixed spaces that will not break over two lines. This is easily done with user-defined macros. For example, `52\dynpercm` typesets as 52 dynes cm⁻¹, providing the following macro definition has been included in the preamble.

```
\newcommand\dynpercm{\nobreak\mbox{\;$\;$dynes\,cm$^{-1}$}}
```

5. User-defined macros

If you define your own macros you must ensure that their names do not conflict with any existing macros in plain T_EX or L^AT_EX (or AMS L^AT_EX if you are using this). You should also place them in the preamble to your input file, between the `\documentclass` and `\begin{document}` commands.

Apart from scanning the indexes of the relevant manuals, you can check whether a macro name is already used in plain T_EX or L^AT_EX by using the T_EX command `show`. For instance, run L^AT_EX interactively and type `\show<macro_name>` at the T_EX prompt. (Alternatively, insert the `\show` command into the preamble of an input file and T_EX it.)

```
* \show\Re
```

produces the following response from T_EX:

```
> \Re=\mathchar"23C.
<*> \show\Re
```

By contrast `\Real` is not part of plain T_EX or L^AT_EX and `\show\Real` generates:

```
> \Real=undefined
<*> \show\Real
```

confirming that this name can be assigned to a user-defined macro.

Alternatively, you can just use `\newcommand`, which will check for the existence of the macro you are trying to define. If the macro exists L^AT_EX will respond with:

```
! LaTeX Error: Command ... already defined.
```

In this case you should choose another name, and try again.

Such macros must be in a place where they can easily be found and modified by the journal's editors or typesetter. They must be gathered together in the preamble of your input file, or in a separate `macros.tex` file with the command `\input{macros}` in the preamble. Macro definitions must not be scattered about your document where they are likely to be completely overlooked by the typesetter.

The same applies to font definitions that are based on Computer Modern fonts. These must be changed by the typesetter to use the journal's T_EX typefaces. In this case, you should draw attention to these font definitions on the hard copy that you submit for publication and by placing a comment in your input file just before the relevant definitions, for example `% replace font!`

6. Some guidelines for using standard facilities

The following notes may help you achieve the best effects with the standard L^AT_EX facilities that remain in the JPP style.

Table 1. An example table

Figure	hA	hB	hC
2	$\exp(\pi ix)$	$\exp(\pi iy)$	0
3	-1	$\exp(\pi ix)$	1
4	$-4 + 3i$	$-4 + 3i$	1.6
5	-2	-2	1.2i

6.1. Sections

\LaTeX provides five levels of section headings, only four of which are defined in the JPP class file:

Heading A – `\section{...}`
 Heading B – `\subsection{...}`
 Heading C – `\subsubsection{...}`
 Heading D – `\paragraph{...}`

There is no `\subparagraph` in the JPP style.

To obtain non-bold in a bold heading use the usual $\LaTeX_{2\epsilon}$ commands for changing typeface; for example `\section{Fluctuations in Ca\textsc{ii}}`.

6.2. Tables

The `table` environment is implemented as described in the \LaTeX manual to provide consecutively numbered floating inserts for tables.

JPP class will cope with most table positioning problems and you should not normally use the optional positional qualifiers `t`, `b`, `h` on the `table` environment, as this would override these decisions. Table captions should appear at the bottom of the table; therefore you should place the `\caption` command before the `\begin{tabular}`.

The JPP `table` environment will insert rules above and below the table as required by the JPP style, so you should not attempt to insert these yourself. The only time you need to intervene with the rules is when two or more tables fall one above another. When this happens, you will get two rules together and too much space between the tables; the solution is to add `\norule` before the end of upper table and `\followon` between tables as shown here:

```

...
\end{center}
\caption{Dimensionless parameters}\label{dimensionless_p}
\norule
\end{table}
\followon
\begin{table}
\begin{center}
...

```

The JPP style dictates that vertical rules should never be used within the body of the table, and horizontal rules should be used only to span columns with the same headings. Extra space can be inserted to distinguish groups of rows or columns.

As an example, table 1 is produced using the following commands:

```

\begin{table}
\caption{An example table} \label{sample-table}

```

```

\begin{center}
\begin{tabular}{cccc}
\hline
{Figure} & {$hA$} & {$hB$} & {$hC$}\\
\hline
2 & $\exp\;(\upi \mathrm{i} x)$ & & \\
& $\exp\;(\upi \mathrm{i} y)$ & & $0$\\
3 & $-1$ & $\exp\;(\upi \mathrm{i} x)$ & $1$\\
4 & $-4+3\mathrm{i}$ & $-4+3\mathrm{i}$ & $1.6$\\
5 & $-2$ & $-2$ & $1.2 \mathrm{i}$
\end{tabular}
\end{center}
\end{table}

```

The `tabular` environment has been modified for the JPP style in the following ways:

- (a) Additional vertical space is inserted above and below a horizontal rule produced by `\hline`
- (b) Tables are centred, and span the full width of the page; that is, they are similar to the tables that would be produced by `\begin{tabular*}{\textwidth}`.
- (c) As with normal L^AT_EX, if a footnote needs to be inserted into the body of the table, the `tabular` environment should be enclosed in a `minipage` environment of width `\textwidth`. e.g.

```

\begin{minipage}{\textwidth}
\begin{tabular}{cccc}
\hline
{Figure} & {$hA$} & {$hB$}\footnote{A table must be
inside a \verb"minipage" environment if it includes
table footnotes.}
& {$hC$}\\
...
\end{tabular}
\end{minipage}

```

Commands to redefine quantities such as `\arraystretch` should be omitted. If the original tabular facilities are needed, there is a new environment ‘`oldtabular`’, which has none of the reformatting; it should be used in exactly the same way.

6.3. Illustrations (or figures)

Artwork for all figures must be supplied separately, to be processed by the Printer, and so L^AT_EX’s `picture` environment, for example, cannot be used. An approximate amount of space should be left, using the `\vspace` command.

The JPP style will cope with most figure positioning problems and you should not normally use the optional positional qualifiers `t`, `b`, `h` on the `figure` environment, as this would override these decisions. Figure captions should be below the figure itself, therefore the `\caption` command should appear after the space left for the illustration within the `figure` environment. For example, figure 1 is produced using the following commands:

Figure 1. An example figure with space for artwork.

```

\begin{figure}
  \vspace{3cm}
  \caption{An example figure with space for artwork.}
  \label{sample-figure}
\end{figure}

```

If a figure caption is too long to fit on the same page as its illustration, the caption may be typeset as ‘FIGURE X. For caption see facing page.’, and the longer caption typeset at the bottom of the facing page. Authors should not concern themselves unduly with such details, and may leave pages long.

6.4. Acknowledgments

Acknowledgments should appear at the close of your paper, just before the list of references and any appendices. Use the `acknowledgments` environment, which simply inserts an ‘Acknowledgments’ subsection heading.

There is also an `acknowledgment` (or `acknowledgement`) environment for typesetting a single acknowledgement.

6.5. Appendices

You should use the standard L^AT_EX `\appendix` command to place any Appendices, normally, just before the references. This numbers appendices as A, B etc. , equations as (A1), (B1) etc. , and figures and tables as A1, B1 etc.

If you have only one Appendix, you should use the `\oneappendix` command (instead of `\appendix`). This command does the same as `\appendix`, except it allows `jpp.cls` to typeset a single Appendix correctly.

6.6. References

As with standard L^AT_EX, there are two ways of producing a list of references; either by compiling a list (using a `thebibliography` or `thereferences` environment), or by using Bib_TE_X with a suitable bibliographic database.

References in the text should follow either the Harvard (name/date) or Vancouver (numbered) system. In the Harvard system, each reference should be cited in the text as ‘author(s) (date)’ or ‘(author(s) date)’, and the reference list at the end of the paper should be in *alphabetical order*. In the Vancouver system, references should be indicated in the text by numbers in square brackets (e.g. [1], [1,2], [1–4], etc.), and should be listed at the end of the paper in *numerical order of citation*. For details of the style of entries within the reference list, please see any recent issue of the journal.

6.6.1. References in the text References in the text are given by author and date like Dennis (1985) or numbered system [12]. Each entry has a key, which is assigned by the author and used to refer to that entry in the text.

6.6.2. *Harvard (name/date)* The following listing shows some references prepared in author (date) style of the journal; the code produces the references at the end of this guide.

```
\begin{thebibliography}{}
  \bibitem[Abramowitz and Stegun (1965)]{AS65}
    {Abramowitz, M. and Stegun, I.\,A.} 1965
    {\em Handbook of Mathematical Functions}. Dover.
  \bibitem[Dennis (1985)]{Den85}
    {Dennis, S.\,C.\,R.} 1985
    Compact explicit finite difference approximations to the
    Navier--Stokes equation. In {\em Ninth Intl Conf. on
    Numerical Methods in Fluid Dynamics\} (ed. Soubbaramayer
    and J.\,P. Boujot). Lecture Notes in Physics, vol. 218,
    pp. 23--51. Springer.
  \bibitem[Jones (1976)]{Jon1976}
    {Jones, O.\,C.} 1976
    An improvement in the calculation of turbulent friction in
    rectangular ducts. {\em Trans. ASME\} J:
    {\em J.\,Fluids Engng\} {\bf 98}, 173--181.
  \bibitem[Saffman (1990)]{Saf1990}
    {Saffman, P.\,G.} 1990
    A model vortex reconnection. {\em J.\,Fluid Mech.}
    {\bf 212}, 395--402.
  \bibitem[Saffman and Schatzman (1982)]{SS1982}
    {Saffman, P.\,G. and Schatzman, J.\,C.} 1982
    Stability of a vortex street of finite vortices.
    {\em J.\,Fluid Mech.} {\bf 117}, 171--185.
  \bibitem[Saffman and Yuen (1980)]{SY1980}
    {Saffman, P.\,G. and Yuen, H.\,C.} 1980
    A new type of three-dimensional deep-water wave of permanent
    form. {\em J.\,Fluid Mech.} {\bf 101}, 797--808.
  \bibitem[Shaqfeh and Koch (1990)]{SK1990}
    {Shaqfeh, E.\,S.\,G. and Koch, D.\,L.} 1990
    Orientational dispersion of fibres in extensional flow.
    {\em Phys. Fluids\} A {\bf 2}, 1077--1081.
  \bibitem[Wijngaarden (1968)]{Wij1968}
    {Wijngaarden, L. van} 1968
    On the oscillations near and at resonance in open pipes.
    {\em J.\,Engng Maths\} {\bf 2}, 225--240
  \bibitem[Williams (1964)]{Wil64}
    {Williams, J.\,A.} 1964
    A nonlinear problem in surface water waves. PhD thesis,
    University of California, Berkeley.
\end{thebibliography}
```

Each entry takes the form

```
\bibitem[Author(s) (Date)]{tag}
  Bibliography entry
```

where **Author(s)** should be the author names as they are cited in the text, **Date** is the date to be cited in the text, and **tag** is the tag that is to be used as an argument for the `\cite{}` command. **Bibliography entry** should be the material that is to appear in the bibliography, suitably formatted.

References

- Abramowitz, M. and Stegun, I. A. 1965 *Handbook of Mathematical Functions*. Dover.
- Dennis, S. C. R. 1985 Compact explicit finite difference approximations to the Navier–Stokes equation. In *Ninth Intl Conf. on Numerical Methods in Fluid Dynamics* (ed. Soubbaramayer and J. P. Boujot). Lecture Notes in Physics, vol. 218, pp. 23–51. Springer.
- Jones, O. C. 1976 An improvement in the calculation of turbulent friction in rectangular ducts. *Trans. ASME J: J. Fluids Engng* **98**, 173–181.
- Saffman, P. G. 1990 A model vortex reconnection. *J. Fluid Mech.* **212**, 395–402.
- Saffman, P. G. and Schatzman, J. C. 1982 Stability of a vortex street of finite vortices. *J. Fluid Mech.* **117**, 171–185.
- Saffman, P. G. and Yuen, H. C. 1980 A new type of three-dimensional deep-water wave of permanent form. *J. Fluid Mech.* **101**, 797–808.
- Shaqfeh, E. S. G. and Koch, D. L. 1990 Orientational dispersion of fibres in extensional flow. *Phys. Fluids A* **2**, 1077–1081.
- Wijngaarden, L. van 1968 On the oscillations near and at resonance in open pipes. *J. Engng Maths* **2**, 225–240
- Williams, J. A. 1964 A nonlinear problem in surface water waves. PhD thesis, University of California, Berkeley.

6.6.3. Vancouver (numbered) system The following listing shows some references prepared in Vancouver (numbered) system style of the journal; the code produces the references at the end of this guide.

```
\begin{thereferences}{9}
  \bibitem{Jon76}
    {Jones, O.\,C.},
    An improvement in the calculation of turbulent friction in
    rectangular ducts. {\em Trans. ASME\}/ J:
    {\em J.\,Fluids Engng\}/ {\bf 98}, 173--181 (1976).
  \bibitem{Saf90}
    {Saffman, P.\,G.},
    A model vortex reconnection. {\em J.\,Fluid Mech.}
    {\bf 212}, 395--402 (1990).
  \bibitem{SS82}
    {Saffman, P.\,G. and Schatzman, J.\,C.},
    Stability of a vortex street of finite vortices.
    {\em J.\,Fluid Mech.} {\bf 117}, 171--185 (1982).
  \bibitem{SY80}
    {Saffman, P.\,G. and Yuen, H.\,C.},
    A new type of three-dimensional deep-water wave of permanent
    form. {\em J.\,Fluid Mech.} {\bf 101}, 797--808 (1980).
  \bibitem{SK90}
    {Shaqfeh, E.\,S.\,G. and Koch, D.\,L.}
    Orientational dispersion of fibres in extensional flow.
    {\em Phys. Fluids\}/ A {\bf 2}, 1077--1081 (1990).
```



```

\bibitem{Wij68}
  {Wijngaarden, L. van},
  On the oscillations near and at resonance in open pipes.
  {\em J.\,Engng Maths\} {\bf 2}, 225--240 (1968).
\end{thereferences}

```

Each entry takes the form

```

\bibitem{tag}
  Bibliography entry

```

where `tag` is the tag that is to be used as an argument for the `\cite{}` command. `Bibliography entry` should be the material that is to appear in the bibliography, suitably formatted.

References

- [1] Jones, O. C., An improvement in the calculation of turbulent friction in rectangular ducts. *Trans. ASME J: J. Fluids Engng* **98**, 173–181 (1976).
- [2] Saffman, P. G., A model vortex reconnection. *J. Fluid Mech.* **212**, 395–402 (1990).
- [3] Saffman, P. G. and Schatzman, J. C., Stability of a vortex street of finite vortices. *J. Fluid Mech.* **117**, 171–185 (1982).
- [4] Saffman, P. G. and Yuen, H. C., A new type of three-dimensional deep-water wave of permanent form. *J. Fluid Mech.* **101**, 797–808 (1980).
- [5] Shaqfeh, E. S. G. and Koch, D. L. Orientational dispersion of fibres in extensional flow. *Phys. Fluids A* **2**, 1077–1081 (1990).
- [6] Wijngaarden, L. van, On the oscillations near and at resonance in open pipes. *J. Engng Maths* **2**, 225–240 (1968).

Appendix A. Special commands in `jpp.cls`

The following is a summary of the new commands, optional arguments and environments which have been added to the standard \LaTeX user-interface in creating the JPP class file.

New commands

<code>\affiliation</code>	use after <code>\author</code> to typeset an affiliation.
<code>\affilskip</code>	use immediately after <code>\</code> in <code>\affiliation</code> to give correct vertical spacing between separate affiliations.
<code>\author</code>	do not use <code>\</code> in <code>\author</code> to start an affiliation.
<code>\followon</code>	to remove space between adjacent tables.
<code>\ls</code>	to letter space the author's name.
<code>\newtheorem</code>	this is enhanced so that you can produce unnumbered versions of the environments by using the <code>*</code> form. e.g. <code>\begin{theorem*}</code> .
<code>\newdefinition</code>	this environment works like the <code>\newtheorem</code> command, except it produces environments which are typeset in roman instead of italic. Again unnumbered 'definitions' can be typeset using the <code>*</code> forms.
<code>\norule</code>	to remove the rule below a table.
<code>\ns</code>	to insert space between an author's names.
<code>\oneappendix</code>	does the same as <code>\appendix</code> , except it allows <code>jpp.cls</code> to typeset a single Appendix correctly.

New optional arguments

<code>[<short title>]</code>	in the <code>\title</code> command: to define a right running headline that is different from the article title.
<code>[<short author>]</code>	in the <code>\author</code> command: to define a left running headline that is different from the authors' names as typeset at the article opening.
<code>[<widest label>]</code>	in <code>\begin{enumerate}</code> : to ensure the correct alignment of numbered lists.

New environments

<code>acknowledg(e)ment(s)</code>	to typeset acknowledgements.
<code>proof</code>	to typeset mathematical proofs.
<code>proof*</code>	to typeset mathematical proofs without the terminating proofbox.
<code>remark</code>	this environment works like the <code>theorem</code> environment; it typesets an italic heading and roman text to contrast with <code>theorem</code> 's small caps heading and italic text.
<code>subeqnarray</code>	enables equation numbers in an array to be numbered as (6.1a), (6.2b), etc.
<code>subequation</code>	enables consecutive equations to be numbered (6.1a), (6.1b), etc.
<code>tabular</code>	has been modified to insert additional space above and below an <code>\hrule</code> and the table caption and body is centred with rules full out across the text measure.

Appendix B. Notes for editors

This appendix contains additional information which may be useful to those who are involved with the final production stages of an article. Authors, who are generally not typesetting the final pages in the journal's typeface (Monotype Modern), do not need this information.

B.0.1. Catchline commands To be placed in the preamble:

- `\date{}`
- `\pagerange{}`
- `\part{}`
- `\pubyear{}`
- `\volume{}`
- `\doi{}`

B.0.2. Footnotes If a footnote falls at the bottom of a page, it is possible for the footnote to appear on the following page (a feature of T_EX). Check for this.

B.0.3. Rules between tables If two or more tables fall one above another, add the commands `\norule` and `\followon` as described in this guide.

B.0.4. Font substitution Check for use of AMS fonts, bold slanted sans serif, and bold math italic and alter preamble definitions to use the appropriate AMS/CUP/Monotype fonts for phototypesetter output.

B.0.5. Font sizes The JPP class file defines all the standard L^AT_EX font sizes. For example:

- `tiny` – This is tiny text.
- `scriptsize` – This is scriptsize text.
- `\indexsize` – This is indexsize text.
- `\footnotesize` – This is footnotesize text.
- `\small` – This is small text.
- `\qsmall` – This is qsmall text (quotations).
- `\normalsize` – This is normalsize text (default).
- `\large` – This is large text.
- `\Large` – This is Large text.
- `\LARGE` – This is LARGE text.

All these sizes are summarized in Table B.1.

Table B.1. Type sizes for L^AT_EX size-changing commands

<i>Size</i>	<i>Size/Baseline</i>	<i>Usage</i>
<code>\tiny</code>	5pt/6pt	–
<code>\scriptsize</code>	7pt/8pt	–
<code>\indexsize</code>	8pt/9pt	catchline.
<code>\footnotesize</code>	9pt/10pt	index, footnotes.
<code>\small</code>	9pt/10pt	‘AND’ in authors’ names, received date, affiliation, figure and table captions.
<code>\qsmall</code>	9.75pt/10.75pt	quote, quotations.
<code>\normalsize</code>	10pt/12pt	main text size, abstract, B and C heads.
<code>\large</code>	11pt/13pt	A head, part no.
<code>\Large</code>	14pt/18pt	part title.
<code>\LARGE</code>	17pt/19pt	article title.
<code>\huge</code>	20pt/25pt	–
<code>\Huge</code>	25pt/30pt	–

An interesting and seminal work on various phenomena in fluid mechanics

ALAN N. OTHER^{1†},
 H.-C. SMITH¹ and J. Q. PUBLIC²

¹Department of Chemical Engineering, University of America, Somewhere, IN 12345, USA

²Department of Aerospace and Mechanical Engineering, University of Camford, Academic Street, Camford, CF3 5QL, UK

(Received 1 July 1994 and in revised form 30 October 1998)

Abstract. Using Stokes flow between eccentric counter-rotating cylinders as a prototype for bounded nearly parallel lubrication flow, we investigate the effect of a slender recirculation region within the flow field on cross-stream heat or mass transport in the important limit of high Péclet number Pe where the enhancement over pure conduction heat transfer without recirculation is most pronounced. The steady enhancement is estimated with a matched asymptotic expansion to resolve the diffusive boundary layers at the separatrices which bound the recirculation region. The enhancement over pure conduction is shown to vary as $\epsilon^{\frac{1}{2}}$ at infinite Pe , where $\epsilon^{\frac{1}{2}}$ is the characteristic width of the recirculation region. The enhancement decays from this asymptote as $Pe^{-\frac{1}{2}}$.

1. Introduction

The use of integral equations to solve exterior problems in linear acoustics, i.e. to solve the Helmholtz equation $(\nabla^2 + k^2)\phi = 0$ outside a surface S given that ϕ satisfies certain boundary conditions on S , is very common. A good description is provided by 9. Integral equations have also been used to solve the two-dimensional Helmholtz equation that arises in water-wave problems where there is a constant depth variation. The problem of wave oscillations in arbitrarily shaped harbours using such techniques has been examined (see for example Hwang & Tuck 1970; Lee 1971).

In a recent paper 8 have shown how radiation and scattering problems for vertical circular cylinders placed on the centreline of a channel of finite water depth can be solved efficiently using the multipole method devised originally by Ursell (1950). This method was also used by 2 to prove the existence of trapped modes in the vicinity of such a cylinder at a discrete wavenumber $k < \pi/2d$ where $2d$ is the channel width.

Many water-wave/body interaction problems in which the body is a vertical cylinder with constant cross-section can be simplified by factoring out the depth dependence. Thus if the boundary conditions are homogeneous we can write the

† Present address: Plasma Physics Inc., 24 The Street, Lagos, Nigeria

velocity potential $\phi(x, y, z, t) = \text{Re}\{\phi(x, y) \cosh k(z + h)e^{-i\omega t}\}$, where the (x, y) -plane corresponds to the undisturbed free surface and z is measured vertically upwards with $z = -h$ the bottom of the channel.

Subsequently Callan *et al.* (1991) proved the existence of, and computed the wavenumbers for, the circular cross-section case. It should be noted however that experimental evidence for acoustic resonances in the case of the circular cylinder is given by Bearman & Graham (1980, pp. 231–232).

6 provided a theory for determining the trapped-mode frequencies for the thin plate, based on a modification of the Wiener–Hopf technique.

The use of channel Green’s functions, developed in §2, allows the far-field behaviour to be computed in an extremely simple manner, whilst the integral equation constructed in §3 enables the trapped modes to be computed in §4 and the scattering of an incident plane wave to be solved in §5. Appendix A contains comparisons with experiments.

2. Green’s functions

2.1. Construction of equations

We are concerned with problems for which the solution, ϕ , is either symmetric or antisymmetric about the centreline of the waveguide, $y = 0$. The first step is the construction of a symmetric and an antisymmetric Green’s function, $G_s(P, Q)$ and $G_a(P, Q)$. Thus we require

$$(\nabla_P^2 + k^2)G_s = (\nabla_P^2 + k^2)G_a = 0 \quad (2.1)$$

in the fluid, where ∇_ρ is a gradient operator, except when $P \equiv Q$,

$$G_s, G_a \sim 1/(2\pi) \ln r \quad \text{as } r \equiv |P - Q| \rightarrow 0, \quad (2.2)$$

$$\frac{\partial G_s}{\partial y} = \frac{\partial G_a}{\partial y} = 0 \quad \text{on } y = d, \quad (2.3)$$

$$\frac{\partial G_s}{\partial y} = 0 \quad \text{on } y = 0, \quad (2.4)$$

$$G_a = 0 \quad \text{on } y = 0, \quad (2.5)$$

and we require G_s and G_a to behave like outgoing waves as $|x| \rightarrow \infty$.

One way of constructing G_s or G_a is to replace (2.1) and (2.2) by

$$(\nabla_P^2 + k^2)G_s = (\nabla_P^2 + k^2)G_a = -\delta(x - \xi)\delta(y - \eta) \quad (2.6)$$

and to assume initially that k has a positive imaginary part.

2.2. Further developments

Using results from 8 we see that this has the integral representation

$$-\frac{1}{2\pi} \int_0^\infty \gamma^{-1} [e^{-k\gamma|y-\eta|} + e^{-k\gamma(2d-y-\eta)}] \cos k(x - \xi)t \, dt, \quad 0 < y, \quad \eta < d, \quad (2.7)$$

where

$$\gamma(t) = \begin{cases} -i(1 - t^2)^{\frac{1}{2}}, & t \leq 1 \\ (t^2 - 1)^{\frac{1}{2}}, & t > 1. \end{cases}$$

In order to satisfy (2.4) we add to this the function

$$-\frac{1}{2\pi} \int_0^\infty B(t) \frac{\cosh k\gamma(d-y)}{\gamma \sinh k\gamma d} \cos k(x-\xi)t \, dt$$

which satisfies (2.1), (2.3) and obtain

$$B(t) = 2e^{-k\gamma d} \cosh k\gamma(d-\eta). \quad (2.8)$$

Thus the function

$$G = -\frac{1}{4}i(H_0(kr) + H_0(kr_1)) - \frac{1}{\pi} \int_0^\infty \frac{e^{-k\gamma d}}{\gamma \sinh k\gamma d} \cosh k\gamma(d-y) \cosh k\gamma(d-\eta) \quad (2.9)$$

satisfies (2.1)–(2.4). By writing this function as a single integral which is even in γ , it follows that G is real.

3. The trapped-mode problem

The unit normal from D to ∂D is $\mathbf{n}_q = (-y'(\theta), x'(\theta))/w(\theta)$. Now $G_a = \frac{1}{4}Y_0(kr) + \widetilde{G}_a$ where $r = \{[x(\theta) - x(\psi)]^2 + [y(\theta) - y(\psi)]^2\}^{\frac{1}{2}}$ and \widetilde{G}_a is regular as $kr \rightarrow 0$. In order to evaluate $\partial G_a(\theta, \theta)/\partial n_q$ we note that

$$\frac{\partial}{\partial n_q} \left(\frac{1}{4}Y_0(kr) \right) \sim \frac{\partial}{\partial n_q} \left(\frac{1}{2\pi} \ln r \right) = \frac{1}{2\pi r^2 w(\theta)} [x'(\theta)(y(\theta) - y(\psi)) - y'(\theta)(x(\theta) - x(\psi))]$$

as $kr \rightarrow 0$. Expanding $x(\psi)$ and $y(\psi)$ about the point $\psi = \theta$ then shows that

$$\begin{aligned} \frac{\partial}{\partial n_q} \left(\frac{1}{4}Y_0(kr) \right) &\sim \frac{1}{4\pi w^3(\theta)} [x''(\theta)y'(\theta) - y''(\theta)x'(\theta)] \\ &= \frac{1}{4\pi w^3(\theta)} [\rho'(\theta)\rho''(\theta) - \rho^2(\theta) - 2\rho'^2(\theta)] \quad \text{as } kr \rightarrow 0. \end{aligned} \quad (3.1)$$

3.1. Computation

For computational purposes we discretize (3.1) by dividing the interval $(0, \pi)$ into M segments. Thus we write

$$\frac{1}{2}\phi(\psi) = \frac{\pi}{M} \sum_{j=1}^M \phi(\theta_j) \frac{\partial}{\partial n_q} G_a(\psi, \theta_j) w(\theta_j), \quad 0 < \psi < \pi, \quad (3.2)$$

where $\theta_j = (j - \frac{1}{2})\pi/M$. Collocating at $\psi = \theta_i$ and writing $\phi_i = \phi(\theta_i)$ etc. gives

$$\frac{1}{2}\phi_i = \frac{\pi}{M} \sum_{j=1}^M \phi_j K_{ij}^a w_j, \quad i = 1, \dots, M, \quad (3.3)$$

where

$$K_{ij}^a = \begin{cases} \partial G_a(\theta_i, \theta_j)/\partial n_q, & i \neq j \\ \partial \widetilde{G}_a(\theta_i, \theta_i)/\partial n_q + [\rho'_i \rho''_i - \rho_i^2 - 2\rho_i'^2]/4\pi w_i^3, & i = j. \end{cases} \quad (3.4)$$

For a trapped mode, therefore, we require the determinant of the $M \times M$ matrix whose elements are

$$\delta_{ij} - \frac{2\pi}{M} K_{ij}^a w_j,$$

to be zero. Table 1 shows a comparison of results obtained from this method using

Table 1. Values of kd at which trapped modes occur when $\rho(\theta) = a$

a/d	$M = 4$	$M = 8$	Callan <i>et al.</i>
0.1	1.56905	1.56905	1.56904
0.3	1.50484	1.50484	1.50484
0.5	1.39128	1.39131	1.39131
0.7	1.32281	1.32287	1.32288
0.9	1.34479	1.35160	1.35185

Figure 1. Trapped-mode wavenumbers, kd , plotted against a/d for three ellipses: -----, $b/a = 0.5$; —, $b/a = 1$; - · -, $b/a = 1.5$.

two different truncation parameters with accurate values obtained using the method of Callan *et al.* (1991).

An example of the results that are obtained from our method is given in figure 1. Figure 2 (*a,b*) shows shaded contour plots of ϕ for these modes, normalized so that the maximum value of ϕ on the body is 1.

3.2. Basic properties

Let

$$\rho_l = \lim_{\zeta \rightarrow Z_l^-(x)} \rho(x, \zeta), \quad \rho_u = \lim_{\zeta \rightarrow Z_u^+(x)} \rho(x, \zeta) \quad (3.5a,b)$$

be the fluid densities immediately below and above the cat's-eyes. Finally let ρ_0 and N_0 be the constant values of the density and the vorticity inside the cat's-eyes, so that

$$(\rho(x, \zeta), \phi_{\zeta\zeta}(x, \zeta)) = (\rho_0, N_0) \quad \text{for } Z_l(x) < \zeta < Z_u(x). \quad (3.6)$$

The Reynolds number Re is defined by $u_\tau H/\nu$ (ν is the kinematic viscosity), the length given in wall units is denoted by $()_+$, and the Prandtl number Pr is set equal to 0.7. In (2.1) and (2.2), τ_{ij} and τ_j^θ are

$$\tau_{ij} = \overline{(\bar{u}_i \bar{u}_j)} - \bar{u}_i \bar{u}_j + \overline{(\bar{u}_i u_j^{SGS} + u_i^{SGS} \bar{u}_j)} + \overline{u_i^{SGS} u_j^{SGS}}, \quad (3.7a)$$

$$\tau_j^\theta = \overline{(\bar{u}_j \bar{\theta})} - \bar{u}_j \bar{\theta} + \overline{(\bar{u}_j \theta^{SGS} + u_j^{SGS} \bar{\theta})} + \overline{u_j^{SGS} \theta^{SGS}}. \quad (3.7b)$$

Figure 2. Shaded contour plots of the potential ϕ for the two trapped modes that exist for an ellipse with $a/d = 1.5$, $b/d = 0.75$. (a) Symmetric about $x = 0$, $kd = 0.96$; (b) antisymmetric about $x = 0$, $kd = 1.398$.

3.2.1. Calculation of the terms The first terms in the right-hand side of (3.5a) and (3.5b) are the Leonard terms explicitly calculated by applying the Gaussian filter in the x - and z -directions in the Fourier space.

The interface boundary conditions given by (2.1) and (2.2), which relate the displacement and stress state of the wall at the mean interface to the disturbance quantities of the flow, can also be reformulated in terms of the transformed quantities. The transformed boundary conditions are summarized below in a matrix form that is convenient for the subsequent development of the theory:

$$Q_C = \begin{bmatrix} -\omega^{-2}V'_w & -(\alpha^t\omega)^{-1} & 0 & 0 & 0 \\ \frac{\beta}{\alpha\omega^2}V'_w & 0 & 0 & 0 & i\omega^{-1} \\ i\omega^{-1} & 0 & 0 & 0 & 0 \\ iR_\delta^{-1}(\alpha^t + \omega^{-1}V''_w) & 0 & -(i\alpha^t R_\delta)^{-1} & 0 & 0 \\ \frac{i\beta}{\alpha\omega}R_\delta^{-1}V''_w & 0 & 0 & 0 & 0 \\ (i\alpha^t)^{-1}V'_w & (3R_\delta^{-1} + c^t(i\alpha^t)^{-1}) & 0 & -(\alpha^t)^{-2}R_\delta^{-1} & 0 \end{bmatrix}. \quad (3.8)$$

\mathbf{S}^t is termed the displacement-stress vector and Q_C the flow-wall coupling matrix. Subscript w in (3.8) denotes evaluation of the terms at the mean interface. It is noted that $V''_w = 0$ for the Blasius mean flow.

3.2.2. Wave propagation in anisotropic compliant layers From (2.1), the fundamental wave solutions to (3.1) and (3.2) for a uniformly thick homogeneous layer in the transformed variables has the form of

$$\boldsymbol{\eta}^t = \hat{\boldsymbol{\eta}}^t \exp[i(\alpha^t x_1^t - \omega t)], \quad (3.9)$$

where $\hat{\boldsymbol{\eta}}^t = \mathbf{b} \exp(i\gamma x_3^t)$. For a non-trivial wave, the substitution of (1.7) into (1.3) and (1.4) yields the following determinantal equation:

$$\text{Det}[\rho\omega^2\delta_{ps} - C_{pqrs}^t k_q^t k_r^t] = 0, \quad (3.10)$$

where the wavenumbers $\langle k_1^t, k_2^t, k_3^t \rangle = \langle \alpha^t, 0, \gamma \rangle$ and δ_{ps} is the Kronecker delta.

4. Torus translating along an axis of symmetry

Consider a torus with axes a, b (see figure 2), moving along the z -axis. Symmetry considerations imply the following form for the stress function, given in body coordinates:

$$\mathbf{f}(\theta, \psi) = (g(\psi) \cos \theta, g(\psi) \sin \theta, f(\psi)). \quad (4.1)$$

Because of symmetry, one can integrate analytically in the θ -direction obtaining a pair of equations for the coefficients f, g in (4.1),

$$f(\psi_1) = \frac{3b}{\pi(2(a+b\cos\psi_1))^{\frac{3}{2}}} \int_0^{2\pi} \frac{(\sin\psi_1 - \sin\psi)(a+b\cos\psi)^{\frac{1}{2}}}{(1-\cos(\psi_1-\psi))(2+\alpha)^{\frac{1}{2}}} d\psi, \quad (4.2)$$

$$\begin{aligned} g(\psi_1) = & \frac{3}{\pi(2(a+b\cos\psi_1))^{\frac{3}{2}}} \int_0^{2\pi} \left(\frac{a+b\cos\psi}{2+\alpha} \right)^{\frac{1}{2}} \left\{ f(\psi) [(\cos\psi_1 - \cos\psi - b\beta_1)S + \beta_1 P] \right. \\ & \times \frac{\sin\psi_1 - \sin\psi}{1-\cos(\psi_1-\psi)} + g(\psi) \left[\left(2+\alpha - \frac{(\sin\psi_1 - \sin\psi)^2}{1-\cos(\psi-\psi_1)} - b^2\gamma \right) S \right. \\ & \left. \left. + \left(b^2 \cos\psi_1\gamma - \frac{a}{b}\alpha \right) F\left(\frac{1}{2}\pi, \delta\right) - (2+\alpha)\cos\psi_1 E\left(\frac{1}{2}\pi, \delta\right) \right] \right\} d\psi, \end{aligned} \quad (4.3)$$

$$\alpha = \alpha(\psi, \psi_1) = \frac{b^2(1-\cos(\psi-\psi_1))}{(a+b\cos\psi)(a+b\cos\psi_1)}; \quad \beta - \beta(\psi, \psi_1) = \frac{1-\cos(\psi-\psi_1)}{a+b\cos\psi}. \quad (4.4)$$

5. Conclusions

We have shown how integral equations can be used to solve a particular class of problems concerning obstacles in waveguides, namely the Neumann problem for bodies symmetric about the centreline of a channel, and two such problems were considered in detail.

Acknowledgements

We would like to acknowledge the useful comments of a referee concerning the solution procedure used in §5. A. N. O. is supported by SERC under grant number GR/F/12345.

Appendix A. Boundary conditions

It is convenient for numerical purposes to change the independent variable in (4.1) to $z = y/\tilde{v}_T^{\frac{1}{2}}$ and to introduce the dependent variable $H(z) = (f - \tilde{y})/\tilde{v}_T^{\frac{1}{2}}$. Equation (4.1) then becomes

$$(1-\beta)(H+z)H'' - (2+H')H' = H'''. \quad (A1)$$

Boundary conditions to (4.3) follow from (4.2) and the definition of H :

$$\left. \begin{aligned} H(0) &= \frac{\epsilon \bar{C}_v}{\tilde{v}_T^{\frac{1}{2}}(1-\beta)}; & H'(0) &= -1 + \epsilon^{\frac{2}{3}} \bar{C}_u + \epsilon \hat{C}'_u; \\ H''(0) &= \frac{\epsilon u_*^2}{\tilde{v}_T^{\frac{1}{2}} u_P^2}; & H'(\infty) &= 0. \end{aligned} \right\} \quad (\text{A } 2)$$

Appendix B

A simple sufficient condition for the method of separation of variables to hold for the convection problem is derived. This criterion is then shown to be satisfied for the ansatz described by (3.27), thus justifying the approach used in §3. The basic ingredient of our argument is contained in the following estimate for a Rayleigh Ritz ratio:

LEMMA 1. *Let $f(z)$ be a trial function defined on $[0, 1]$. Let Λ_1 denote the ground-state eigenvalue for $-d^2g/dz^2 = \Lambda g$, where g must satisfy $\pm dg/dz + \alpha g = 0$ at $z = 0, 1$ for some non-negative constant α . Then for any f that is not identically zero we have*

$$\frac{\alpha(f^2(0) + f^2(1)) + \int_0^1 \left(\frac{df}{dz}\right)^2 dz}{\int_0^1 f^2 dz} \geq \Lambda_1 \geq \left(\frac{-\alpha + (\alpha^2 + 8\pi^2\alpha)^{\frac{1}{2}}}{4\pi}\right)^2. \quad (\text{B } 1)$$

Before proving it, we note that the first inequality is the standard variational characterization for the eigenvalue Λ_1 .

COROLLARY 1. *Any non-zero trial function f which satisfies the boundary condition $f(0) = f(1) = 0$ always satisfies*

$$\int_0^1 \left(\frac{df}{dz}\right)^2 dz. \quad (\text{B } 2)$$

References

Bearman, P. W. & Graham, J. M. R. 1980 Vortex shedding from bluff bodies in oscillating flow: A report on Euromech 119. *J. Fluid Mech.* **99**, 225–245.

Callan, M., Linton, C. M. & Evans D. V. 1991 Trapped modes in two-dimensional waveguides. *J. Fluid Mech.* **229**, 51–64.

Dennis, S. C. R. 1985 Compact explicit finite difference approximations to the Navier–Stokes equation. In *Ninth Intl Conf. on Numerical Methods in Fluid Dynamics* (ed. Soubbaramayer & J. P. Boujot). Lecture Notes in Physics, vol. 218, pp. 23–51. Springer.

Hwang, L.-S. & Tuck, E. O. 1970 On the oscillations of harbours of arbitrary shape. *J. Fluid Mech.* **42**, 447–464.

Keller, H. B. 1977 Numerical solution of bifurcation and nonlinear eigenvalue problems. In *Applications of Bifurcation Theory* (ed. P. H. Rabinovich), pp. 359–384. Academic.

Koch, W. 1983 Resonant acoustic frequencies of flat plate cascades. *J. Sound Vib.* **88**, 233–242.

- Lee, J.-J. 1971 Wave-induced oscillations in harbours of arbitrary geometry. *J. Fluid Mech.* **45**, 375–394.
- Linton, C. M. & Evans, D. V. 1992 The radiation and scattering of surface waves by a vertical circular cylinder in a channel. *Phil. Trans. R. Soc. Lond. A* **338**, 325–357.
- Martin, P. A. 1980 On the null-field equations for the exterior problems of acoustics. *Q. J. Mech. Appl. Maths* **33**, 385–396.
- Rogallo, R. S. 1981 Numerical experiments in homogeneous turbulence. *NASA Tech. Mem.* 81835.
- Wijngaarden, L. van 1968 On the oscillations near and at resonance in open pipes. *J. Engng Maths* **2**, 225–240.
- Williams, J. A. 1964 A nonlinear problem in surface water waves. PhD thesis, University of California, Berkeley.

References

- [1] Bearman, P. W. & Graham, J. M. R. 1980 Vortex shedding from bluff bodies in oscillating flow: A report on Euromech 119. *J. Fluid Mech.* **99**, 225–245.
- [2] Callan, M., Linton, C. M. & Evans D. V. 1991 Trapped modes in two-dimensional waveguides. *J. Fluid Mech.* **229**, 51–64.
- [3] Dennis, S. C. R. 1985 Compact explicit finite difference approximations to the Navier–Stokes equation. In *Ninth Intl Conf. on Numerical Methods in Fluid Dynamics* (ed. Soubbaramayer & J. P. Boujot). Lecture Notes in Physics, vol. 218, pp. 23–51. Springer.
- [4] Hwang, L.-S. & Tuck, E. O. 1970 On the oscillations of harbours of arbitrary shape. *J. Fluid Mech.* **42**, 447–464.
- [5] Keller, H. B. 1977 Numerical solution of bifurcation and nonlinear eigenvalue problems. In *Applications of Bifurcation Theory* (ed. P. H. Rabinovich), pp. 359–384. Academic.
- [6] Koch, W. 1983 Resonant acoustic frequencies of flat plate cascades. *J. Sound Vib.* **88**, 233–242.
- [7] Lee, J.-J. 1971 Wave-induced oscillations in harbours of arbitrary geometry. *J. Fluid Mech.* **45**, 375–394.
- [8] Linton, C. M. & Evans, D. V. 1992 The radiation and scattering of surface waves by a vertical circular cylinder in a channel. *Phil. Trans. R. Soc. Lond. A* **338**, 325–357.
- [9] Martin, P. A. 1980 On the null-field equations for the exterior problems of acoustics. *Q. J. Mech. Appl. Maths* **33**, 385–396.
- [10] Rogallo, R. S. 1981 Numerical experiments in homogeneous turbulence. *NASA Tech. Mem.* 81835.
- [11] Wijngaarden, L. van 1968 On the oscillations near and at resonance in open pipes. *J. Engng Maths* **2**, 225–240.
- [12] Williams, J. A. 1964 A nonlinear problem in surface water waves. PhD thesis, University of California, Berkeley.

